remote sensing

Article

Analysis of Vegetation Cover Change in the Geomorphic Zoning of the Han River Basin Based on Sustainable Development

Yuqing Xiong [1,2], Zizheng Zhang [3], Meichen Fu [1], Li Wang [2], Sijia Li [1], Cankun Wei [1] and Lei Wang [2,4,*]

1 School of Land Science and Technology, China University of Geosciences, Beijing 100083, China; xiongyq@email.cugb.edu.cn (Y.X.); fumeichen@cugb.edu.cn (M.F.); weicankun@email.cugb.edu.cn (C.W.)
2 State Key Laboratory of Remote Sensing Science, Aerospace Information Research Institute, Chinese Academy of Sciences, Beijing 100101, China; wangli@radi.ac.cn
3 College of Resources and Environment, Hubei University, Wuhan 430062, China; zzz@hubu.edu.cn
4 International Research Center of Big Data for Sustainable Development Goals, Beijing 100094, China
* Correspondence: wanglei@radi.ac.cn

Abstract: The Han River Basin, a critical water conservation and ecological barrier in Hubei Province, is intricately associated with the United Nations Sustainable Development Goals (SDGs). Research results show that vegetation cover changes are affected by multiple factors, and understanding the influences of climate change and human activities on vegetation is imperative for achieving sustainable development in the basin. Through quantitative assessment of vegetation changes in diverse landform regions, implementing adaptive ecological construction and environmental protection will foster the sustainable development of ecological civilization in the Han River Basin. This study utilizes MODIS13Q1 data and employs diverse analytical methods to investigate the characteristics of vegetation change and the interrelationships between climate change, meteorological factors, and vegetation cover in various geomorphological areas of the Han River Basin from 2000 to 2020. The results showed that (1) throughout the entire study period, the *NDVI* of the six types of geomorphological divisions in the Han River Basin exhibited a fluctuating upward trend, with the changes in the low-altitude hilly geomorphic regions being particularly noteworthy. (2) Within the study area, approximately 92.67% of vegetation coverage displayed an increasing trend, while 7.33% showed degradation, predominantly in plains and platforms. Notably, the area of continuous improvement (31.16%) outweighed the area of continuous degradation (3.05%), with low and middle-relief mountain areas demonstrating the most robust growth and sustainability. (3) Human agriculture activities and urbanization processes have emerged as the primary driving force behind vegetation changes in the Han River Basin. The responses of vegetation to climate change and human activities exhibited significant variations across diverse geomorphological regions. In areas characterized by vegetation improvement, the contribution rate of human activities to *NDVI* changes in different vegetation types surpassed 70%, with plain areas displaying the highest contribution rate at a remarkable 90%. In contrast, the plain and platform regions of the vegetation degradation area were significantly influenced by climate change. In future watershed ecological environment management, it is essential to not only recognize the dominant role of human activities in promoting the growth of mountain vegetation *NDVI* but also address the impact of climate change on the degradation of vegetation *NDVI* in plains and platforms. A comprehensive understanding of these factors is crucial for devising effective strategies to ensure sustainable development and ecological balance in the Han River Basin.

Keywords: sustainable development goals; Han River Basin; geomorphic zoning; vegetation coverage

Citation: Xiong, Y.; Zhang, Z.; Fu, M.; Wang, L.; Li, S.; Wei, C.; Wang, L. Analysis of Vegetation Cover Change in the Geomorphic Zoning of the Han River Basin Based on Sustainable Development. *Remote Sens.* **2023**, *15*, 4916. https://doi.org/10.3390/rs15204916

Academic Editor: Dino Ienco

Received: 23 August 2023
Revised: 20 September 2023
Accepted: 26 September 2023
Published: 11 October 2023

1. Introduction

Vegetation, being a crucial component of terrestrial ecosystems, plays a pivotal role in global soil conservation, climate regulation, hydrological processes, carbon cycling, and ecosystem stabilization. Its dynamic characteristics not only reflect the state of terrestrial ecosystems but also serve as a sensitive indicator of how ecosystems respond to climate change and human activities, providing insights into the overall ecological environment [1–5]. The alterations in vegetation's spatial and temporal patterns have far-reaching implications, transforming not only regional landscape patterns and functions but also influencing ecosystem structures [6]. A large number of studies have shown that vegetation cover changes are affected by multiple factors, mainly climate change and human activities [5,7,8]. Scholars have turned their attention to the crucial topics of vegetation change and its dynamic response to climate fluctuations and human interventions [5,9]. Conducting long-term dynamic monitoring of vegetation growth and transformations, alongside quantitatively assessing the impacts of climate-related factors and human activities on the evolution of terrestrial ecosystems, holds paramount importance. In most areas of China, an increase in temperature will promote an increase in vegetation coverage; an appropriate increase in precipitation can also promote vegetation development [10]. These phenomena serve as pivotal indicators for gauging trends in ecological environmental changes, providing essential guidance for scientific planning and decision-making in the comprehensive management of regional ecological environments [11,12].

The 2030 Agenda for Sustainable Development was formally adopted during the United Nations Sustainable Development Summit in September 2015, comprising 17 global sustainable development goals and 169 specific targets that encompass social, economic, and environmental dimensions. Among the myriad of critical goals outlined in the agenda, there is a particular emphasis on understanding and mitigating the impacts of climate change and human activities on vegetation dynamics. Sustainable Development Goals 13 (SDGs13) and 15 (SDGs15) hold pivotal importance in this realm. This goal urges global cooperation in halting deforestation, restoring degraded lands, conserving biodiversity, and combating desertification and land degradation. As a result, research focused on vegetation change within the context of SDGs13 and SDGs15 is gaining increasing attention from scholars and policymakers alike. Understanding how climate change and human activities impact vegetation dynamics is crucial for guiding informed decisions, implementing effective mitigation strategies, and devising sustainable land use practices [13,14]. By comprehensively analyzing the changes in vegetation patterns, researchers can assess the health and resilience of terrestrial ecosystems, and evaluate the progress towards meeting the objectives set by SDGs13 and SDGs15.

Compared with traditional data, remote sensing big data have advantages such as lower acquisition costs, extended time series, comprehensive spatial coverage, and objective outcomes [14–16]. Long-term remote sensing data with high temporal and spatial resolution have become the primary data source for studying vegetation change due to the continuous development of remote sensing technology [17]. Extracting the multiscale features from high spatial resolution images is one major application area that researchers are working on, especially in remotely sensed applications [18]. Among various vegetation indices, the normalized difference vegetation index (*NDVI*) is considered the best indicator for reflecting vegetation growth status. *MODIS NDVI* has higher spatial resolution and widespread scholarly usage [19,20]. In recent years, many scholars at home and abroad have conducted in-depth research on the spatiotemporal variation of surface vegetation and its driving factors at different temporal and spatial scales based on long-term *NDVI* datasets [21–23]. The results showed that vegetation growth was closely related to climatic conditions, and the response of *NDVI* to climate had large spatial differences in different regions. Insufficient precipitation in arid and semi-arid regions became the key condition restricting vegetation growth. In humid areas, the increase in precipitation leads to a decrease in air temperature which inhibits the growth of vegetation [24,25]. The impact of temperature on vegetation will also vary with different regions. In high latitudes and mountainous areas, the continuous increase in temperature can prolong the growth period of vegetation and promote the growth of vegetation. However, in low- and middle-latitude, arid, and semi-arid regions, rising temperatures will aggravate drought and inhibit vegetation growth [26–28]. In addition to climate change, human activities also have a significant impact on vegetation changes. With the rapid economic development, urban expansion, and the increase in agricultural activity intensity, vegetation growth space is encroached upon, leading to a series of environmental problems such as land degradation, desertification, and soil erosion [29,30]. Since the 1990s, the state has successively implemented a series of ecological construction projects such as returning farmland to forest (grassland), natural forest protection, and soil and water conservation, which has increased vegetation coverage [31].

The spatiotemporal heterogeneity and complexity of vegetation dynamics are further exacerbated by the temporal and spatial differences in climate change and human activities, along with their interactions [32]. While dynamic responses of vegetation to climate change and human activities have been extensively studied on various scales [32–34], most studies tend to focus on vegetation change and its response to precipitation and temperature, neglecting the effects of other meteorological variables, such as radiation, humidity, and wind speed [35–38]. Since the impact of human activities is difficult to quantify, most studies on human activities use qualitative descriptions [33,35,39–42]. Academic research on vegetation cover has primarily centered around the intertwined impacts of climate change and human activities. Despite significant advancements in this area, the driving mechanism behind vegetation dynamics remains unclear. Consequently, there is a growing need to quantitatively assess the influence of climate change and human activities on vegetation growth, which represents a novel research focus. Moreover, there is still a requirement for further exploration regarding the relative contribution rates of various factors to vegetation change. Thus, investigating the relative importance of different drivers in shaping vegetation dynamics remains an important area for future exploration [38,40,42,43]. Landforms play a crucial role in shaping the dynamics of natural elements, including climate and vegetation, at various scales. Consequently, they exert a significant influence on the differentiation of the natural environment. Furthermore, the distinct interplay between human activities and climate change results in notable spatial variations in vegetation across different types of landforms [44–46].

Consequently, the primary objective of this study is to shed light on the spatiotemporal dynamics of vegetation in the Han River Basin and comprehensively examine its response to both climate change and human activities. This analysis can facilitate the implementation of tailored ecological construction and environmental protection measures that align with the specific landform conditions within the basin. The Han River Basin holds crucial importance as an essential ecological security barrier, water conservation area, and biodiversity protection zone in the country. Moreover, it is a critical water source for the South-to-North Water Diversion Middle Route Project, further emphasizing its ecological significance [4]. Existing research on *NDVI* in the Han River Basin has primarily concentrated on exploring the impact of meteorological factors, such as temperature and precipitation [47–49]. However, there has been limited investigation into the influence of diverse landforms, climate change, and human activities on vegetation dynamics in the region [50–52]. Given these critical aspects, further research and collaborative efforts are required to devise effective strategies for sustaining the delicate balance between natural ecosystems and human activities, ensuring harmonious coexistence and promoting the well-being of both the environment and society.

2. Materials and Methods

2.1. Study Area

The Han River originates at the southern foot of the Qinling Mountains in Shaanxi Province and traverses through Shaanxi and Hubei Provinces before merging with the Yangtze River at the Dragon King Temple in Hankou, Wuhan. Being the largest tributary of the Yangtze, the Han River boasts a total length of 1577 km, and covers an extensive area of approximately 159,000 square miles. Its geographical coordinates range from 106°15′E to 114°20′E longitude and 30°10′N to 34°20′N latitude. The Han River Basin experiences a subtropical monsoon climate, with an average annual precipitation of 804 mm and an annual average temperature ranging between 12 and 16 °C. The region's geomorphology is intricate, characterized by significant topographic variations. The southeastern part predominantly comprises plains and platforms, while the northwestern section features a distribution of mountains and hills [53]. Since 1999, the Han River Basin has implemented a range of ecological construction projects, including initiatives like returning farmland to forest and grass, natural forest protection, and soil and water conservation. As a result of these efforts, the ecological environment of the Han River Basin has witnessed significant improvements. However, despite these positive developments, the middle and lower reaches of the basin have experienced rapid urbanization, which has led to increased fragility in the ecological environment of certain areas.

2.2. Data Sources

The *NDVI* data utilized in this research were sourced from the MOD13Q1 *NDVI* dataset, a part of the land products provided by NASA (https://ladsweb.modaps.eosdis.nasa.gov/, accessed on 28 June 2023). This dataset originates from the MODIS sensor aboard the Terra satellite, featuring a spatial resolution of 250 m and a temporal resolution of 16 days. The study period spans from February 2000 to December 2020. For data processing, the MODIS Reprojection Tools software was employed to conduct batch format conversion, projection conversion, and stitching procedures, along with other necessary correction processes. Additionally, data pixel reliability datasets were integrated, and the *NDVI* time series were subjected to Maximum Value Composite analysis to mitigate interference from clouds, atmosphere, and solar altitude angles. The monthly *NDVI* data were then synthesized using ENVI 5.1 software. To create the vegetation growth season *NDVI* dataset for the Han River Basin between 2000 and 2020, vegetation *NDVI* data from April to October was synthesized following the meteorological division standards. This approach ensures a comprehensive and accurate representation of vegetation dynamics within the region during the specified time frame.

The meteorological data used in this study were obtained from the daily value dataset provided by the China Meteorological Data Service Center (https://data.cma.cn/, accessed on 5 March 2023). Initially, data from 92 meteorological stations (Figure 1b) within and around the study area were selected. Subsequently, the daily data were aggregated into monthly data, encompassing five key factors: temperature, precipitation, relative humidity, wind speed, and sunshine. For spatial interpolation, the thin plate smoothing spline (TPS) method from Anusplin 4.2 was employed, yielding a spatial resolution of 250 m. This interpolation technique utilizes the digital elevation model (DEM) as a covariate, effectively accounting for the variations in temperature and precipitation associated with altitude gradients. As a result, the TPS approach ensures higher accuracy and smoother interpolations [54]. Moreover, irradiance data were calculated based on solar climate data, following the solar energy assessment method. This enabled the assessment of solar irradiance, a crucial factor in understanding the impact of solar energy on the study area.

The geomorphological divisions utilized in this study are derived from the 1:1,000,000 Chinese geomorphological map compiled by the Institute of Geographic Sciences and Natural Resources Research, Chinese Academy of Sciences in 2011 [55,56]. The distribution data of the geomorphic types are sourced from the "Geomorphic Atlas of the People's Republic of China (1:1 million)", which subdivides the region into 26 categories based on altitude, degree of relief, and genetic types. For this research, these data were merged, reclassified, and ultimately grouped into six distinct landform types (Table 1): plains, terraced platforms, hills, low-relief mountains (LRM), middle-relief mountains (MRM), and high-relief mountains (HRM). The types distribution is shown in Figure 1c. The information regarding landform types is obtained from the Resource and Environmental Science and Data Center of the Chinese Academy of Sciences (http://www.resdc.cn/, accessed on 28 June 2023). The delineation of the Han River Basin boundary is derived from the Yangtze

River Basin 1:250,000 three-level watershed classification data set provided by the National Earth System Science Data Center (http://www.geodata.cn/, accessed on 28 June 2023).

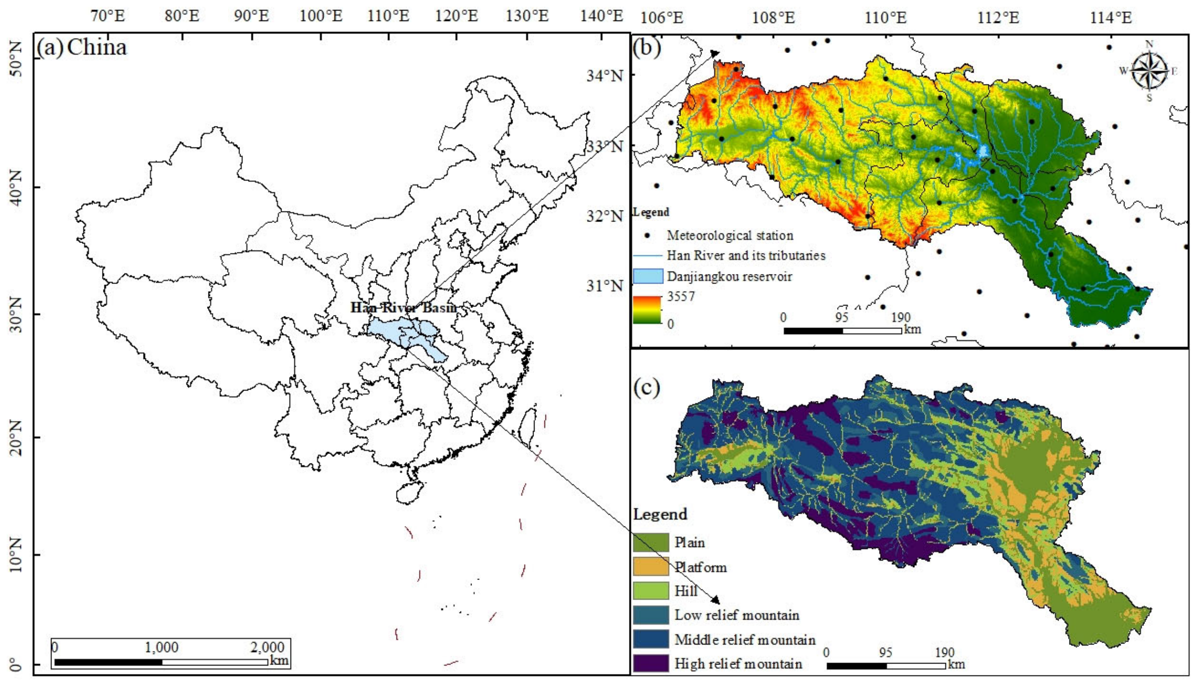

Figure 1. (**a**) Location map of the study area; (**b**) weather stations and terrain; (**c**) landform type distribution.

Table 1. Classification of the basic terrestrial geomorphologic types of the study area.

Altitude Relief	Low Altitude (<1000 m)	Middle Altitude (1000–3500 m)	High Altitude (3500–5000 m)
Plain (<30 m)	Low-altitude plain	Middle-altitude plain	——
Platform (>30 m)	Low-altitude platform	Middle-altitude platform	——
Hill (<200 m)	Low-altitude hill	Middle-altitude hill	——
Low-relief mountain (200–500 m)	Low-relief low-altitude mountain	Low-relief middle-altitude mountain	——
Middle-relief mountain (500–1000 m)	Middle-relief low-altitude mountain	Middle-relief middle-altitude mountain	——
High-relief mountain (1000–2500 m)	——	High-relief middle-altitude mountain	——

Notes: "—" no geomorphologic type represented in the study area.

2.3. Methodology

2.3.1. Theil–Sen Trend Analysis and Mann–Kendall Significance Test

The Theil–Sen trend analysis method is a non-parametric statistical trend analysis method that is not affected by outliers, and does not require data to obey a normal distribution. It is often used to analyze the changing trend of long-term series data such as meteorology, hydrology, and vegetation *NDVI* [57]. By calculating the slope between two groups of data in the series, and taking the median of the slopes of all groups as the overall trend of the time series, it is gradually applied to the long-term analysis of vegetation [58].

$$\beta = median\left(\frac{x_i - x_j}{i - j}\right), \forall j > i \quad (1)$$

where *median* is the median function; x_i and x_j are sequence data; i and j are time series data. If $\beta > 0$, it means that the time series shows an upward trend; otherwise, the time series shows a downward trend.

In this paper, the Mann–Kendall method can be used to test whether the trend is significant [59,60], and the calculation formula is as follows:

$$S = \sum_{i}^{n-1} \sum_{j=i+1}^{n} sgn(x_j - x_i) \tag{2}$$

$$sgn(x_j - x_i) = \begin{cases} +1, & x_j - x_i > 0 \\ 0, & x_j - x_i = 0 \\ -1, & x_j - x_i < 0 \end{cases} \tag{3}$$

$$Z_c = \begin{cases} \frac{S-1}{\sqrt{Var(S)}}, & if\ S > 0 \\ 0, & if\ S = 0 \\ \frac{S+1}{\sqrt{Var(S)}}, & if\ S < 0 \end{cases} \tag{4}$$

where S is the test statistic; Z_c is the standardized test statistic; x_i and x_j are time series data; n is the number of sequence samples.

$$Var(S) = \frac{n(n-1)(2n+5)}{18} \tag{5}$$

Combined with the trend represented by the β value, the significance of the *NDVI* change trend was compared with the significance index, and the significance levels $P_{0.01}$ and $P_{0.05}$ were selected as the critical values, which were comprehensively divided into 6 levels, as shown in Table 2:

Table 2. Trend analysis grading standards.

Trend of *NDVI*	β	Z_c	Trend of *NDVI*	β	Z_c
Highly significant reduction	$\beta < 0$	$\lvert Z_c \rvert > 2.58$	No significant increase	$\beta \geq 0$	$0 > \lvert Z_c \rvert > 1.96$
Significant reduction	$\beta < 0$	$1.96 > \lvert Z_c \rvert \geq 2.58$	Significant increase	$\beta \geq 0$	$1.96 > \lvert Z_c \rvert \geq 2.58$
No significant reduction	$\beta < 0$	$0 > \lvert Z_c \rvert > 1.96$	Highly significant increase	$\beta \geq 0$	$\lvert Z_c \rvert > 2.58$

2.3.2. Hurst Index Analysis

The Hurst index can quantitatively describe the dependence of variables on the time series and judge the time trend. The Hurst exponent based on the rescaled range analysis method (R/S) is an effective method to quantitatively describe the information dependence of non-constant long-period sequences. It is widely used in trend prediction of time series information in fields such as meteorology and hydrology. In recent years, it has also been gradually applied to the analysis of changes in *NDVI* and vegetation net primary productivity. The specific calculation method can refer to relevant research [61,62]. The formula is as follows:

$$\frac{R(T)}{S(T)} = (mT)^H \tag{6}$$

$$R(T) = \max_{1 \leq t \leq T} X(t,T) - \min_{1 \leq t \leq T} X(t,T) \tag{7}$$

$$S(T) = \sqrt{\frac{1}{T} \sum_{t=1}^{T} \left(NDVI_T - \overline{NDVI_T}\right)^2} \tag{8}$$

$$X(t,T) = \sum_{t=1}^{T} \left(NDVI_t - \overline{NDVI_T} \right) \tag{9}$$

$$\overline{NDVI_T} = \frac{1}{T} \sum_{t=1}^{T} NDVI_x \tag{10}$$

where H is Hurst index; $R(T)$ is a range sequence; $S(T)$ is the standard deviation sequence; m is a constant whose value is 1; $X(t,T)$ is the cumulative deviation; $NDVI_t$ $(t = 1,\ 2,\ \ldots, n)$ is *NDVI* time series; $NDVI_T(T = t, t+1, \ldots, n)$ is $NDVI_t$ mean value series.

The value range of the Hurst index is between 0 and 1. When $H = 0.5$, the future change has nothing to do with the past change. When $0.5 < H < 1$, it means that the future trend is consistent with the past trend, and the closer the H value is to 1, the stronger the persistence. When $0 < H < 0.5$, the future trend is opposite to the past trend, and the closer H is to 0, the stronger the anti-persistence.

2.3.3. Correlation Analysis

Correlation analysis is mainly used to reflect the degree and direction of correlation between elements. This study mainly uses pixel-based correlation analysis, using correlation coefficients to express the correlation between *NDVI* and meteorological factors [63]. The formula is as follows:

$$R_{xy} = \frac{\sum_{i=1}^{n} (x_i - \overline{x})(y_i - \overline{y})}{\sqrt{\sum_{i=1}^{n} (x_i - \overline{x})^2 \sum_{i=1}^{n} (y_i - \overline{y})^2}} \tag{11}$$

where x and y are the n-year averages of the two variables; R_{xy} is the simple correlation coefficient between the two elements; n is the sample size. The significance test of the partial correlation coefficient was completed using the Student's t-test method.

2.3.4. Multiple Regression Residual Analysis

Previous studies predominantly employed linear regression and correlation analyses to investigate the influence of climate and human activity on vegetation dynamics. Nevertheless, linear assumptions do not universally apply [8,64]. The residual analysis method, a widely utilized quantitative technique, excels in discerning the contributions of human activity and climate factors to regional vegetation dynamics [27,65]. The impact and relative contribution of human activities and climate change on vegetation *NDVI* changes were studied using the multiple regression residual analysis method [63,66,67]. To quantify human activity factors, this study mainly uses the residual analysis method. It is important to distinguish vegetation changes caused by human activities from those caused by climate change. First, the multiple regression analysis method is used to calculate the predicted $NDVI_{CC}$, which can represent the impact of climate change. Then, the calculated difference between $NDVI_{OBC}$ and $NDVI_{CC}$ is the $NDVI$ residual ($NDVI_{HA}$) that represents the dynamic response of vegetation to human activities [68].

This method mainly has the following three steps: (1) Based on *NDVI* and interpolated temperature and precipitation time series data, with $NDVI$ as the dependent variable and temperature, precipitation, relative humidity, radiation, and wind speed as independent variables, a binary linear regression model was established to calculate the parameters in the model. (2) Based on temperature, precipitation, relative humidity, radiation and wind speed data and the parameters of the regression model, the predicted value of *NDVI* ($NDVI_{CC}$) is calculated to represent the impact of climate factors on vegetation *NDVI* [68]. (3) The difference between the observed $NDVI$ value and $NDVI_{CC}$, that is, the *NDVI* residual ($NDVI_{HA}$), is calculated, which is then used to represent the impact of human activities on vegetation *NDVI* [27,68–70]. The formula is as follows:

$$NDVI_{CC} = a \times Pre + b \times TEM + c \times Rs + d \times Rhu + e \times Wins + f \tag{12}$$

$$NDVI_{HA} = NDVI_{OBS} - NDVI_{CC} \tag{13}$$

$$NDVI_{slope} = \frac{n \times \sum_{i=1}^{n}(i \times NDVI_i) - (\sum_{i=1}^{n} i)(\sum_{i=1}^{n} NDVI_i)}{n \times \sum_{i=1}^{n} i^2 - (\sum_{i=1}^{n} i)^2} \tag{14}$$

where a, b, c, d and e are the regression coefficients of $NDVI$ and precipitation, temperature, total radiation, relative humidity and mean wind speed, respectively; f is a constant; Pre is the annual precipitation; TEM is the annual mean temperature; $NDVI_{CC}$ is the predicted value of the multiple regression equation; $NDVI_{OBS}$ is the actual observed value; $NDVI_{HA}$ is the difference between the observed value and the predicted value, representing the impact of human activities on $NDVI$; $NDVI_{slope}$ is the slope of the linear regression equation; i is the time variable; n is the number of years; $NDVI_i$ is the $NDVI$ value dominated by human activities or climate change.

3. Results

3.1. Vegetation Coverage NDVI Trend Changes in the Study Area

From 2000 to 2020, the *NDVI* of the growing season vegetation in the Han River Basin exhibited a fluctuating growth trend, increasing from 0.651 to 0.737. The annual growth rate was calculated as 13.21% with a growth rate of 0.0038 per year. The highest *NDVI* value was recorded in 2015, while the lowest was observed in 2001 (Figure 2). The *NDVI* of the Han River Basin in the growing season from 2000 to 2020 mainly presents four stages of characteristics: (1) From 2001 to 2002, the *NDVI* of the Han River Basin showed a sudden change from 0.646 to 0.678. The main reason was that China started to implement the natural forest protection project and the project of returning farmland to the forest in 2001. (2) From 2003 to 2010, the *NDVI* fluctuation of the vegetation in the Han River Basin increased. The main reason is that the implementation of soil and water conservation policies and ecological engineering construction in the Han River Basin has achieved certain results, which have a certain restoration and protection effect on the vegetation in the Han River Basin. (3) From 2011 to 2015, the fluctuation of the growing season in the basin increased, mainly because the construction of the middle route project of the South-to-North Water Diversion Project had an impact on the basin environment, which further affected the *NDVI* of the basin during the growing season. (4) The reason may be related to the implementation of the development strategy of the Yangtze River Economic Belt "to step up conservation of the Yangtze River and stop its over development", and the comprehensive protection and restoration of the ecological environment of the Han River.

The *NDVI* of different landform regions of the Han River showed a fluctuating upward trend in the growing season. But there are certain spatial differences. The overall situation follows a certain trend: HRM> MRM > LRM > Whole Basin >Hills > Platforms > Plains. The high undulating mountains are affected by the endowment of vegetation resources, and the original vegetation is in good condition. The average value of vegetation *NDVI* in the growing season is 0.816; it is much higher than the average level of the watershed and other landform divisions. Vegetation change rates in plains and platforms were 1.56%/10 a and 2.93%/10 a, both of which were lower than the basin average (3.78%/10 a), respectively. The main reason is that plains and platforms have less relief and are mostly located in the lower reaches of the river basin. Due to the influence of the cultivated land red line policy and urbanization, the land use types are mostly maintained as cultivated land or transformed into construction land, so the growth rate of vegetation coverage is relatively low. Due to the implementation of the project of returning farmland to forest and grassland in low-relief mountainous and hilly areas, the cultivated land has been restored to forest land, and there is a large room for vegetation growth.

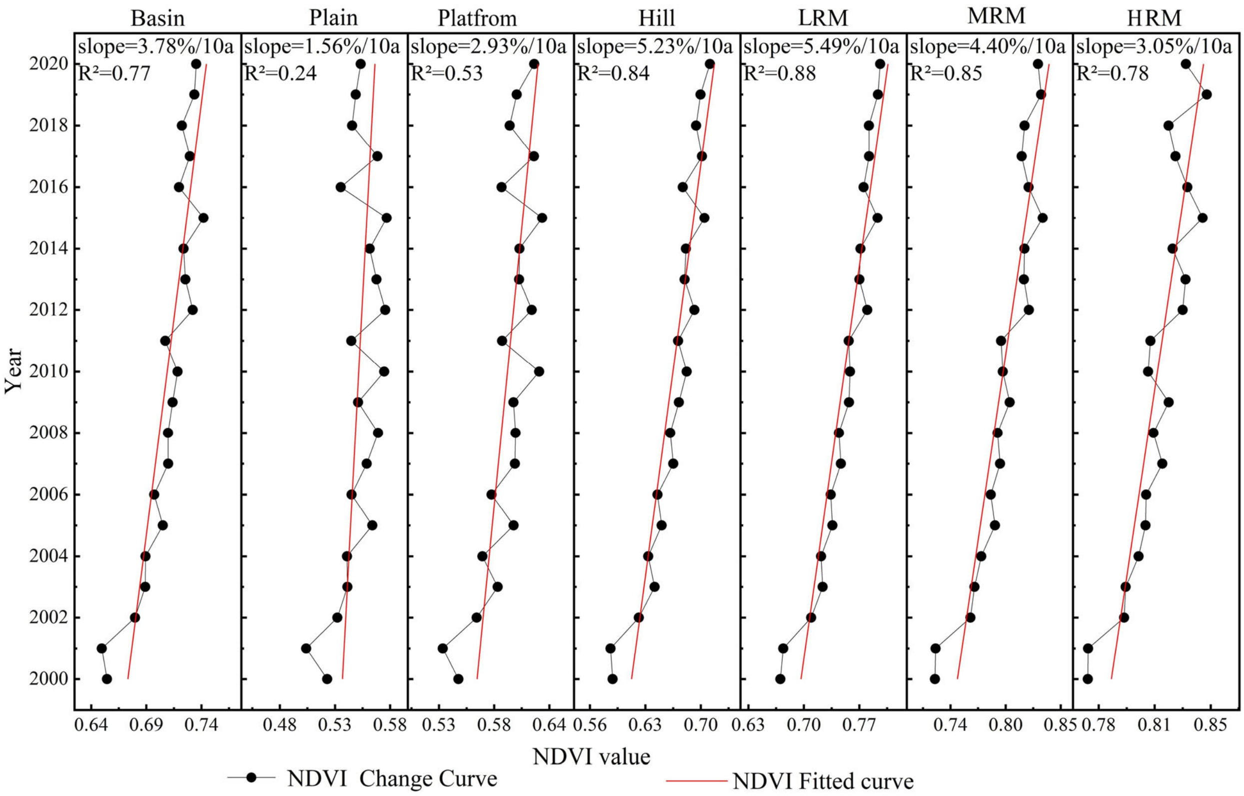

Figure 2. Vegetation change characteristics in the Han River Basin and geomorphic zones from 2000 to 2020.

3.2. Spatial Variation Trend Characteristics of Vegetation Coverage

The *NDVI* change trend for vegetation cover in the Han River Basin reveals highly significant increases and significant increases, accounting for 64.90% and 10.64%, respectively. Conversely, the remaining areas show extremely significant decreases (0.93%) and significant decreases (0.83%), indicating the overall favorable condition of vegetation coverage in the region. The area experiencing vegetation improvement is steadily increasing, while the degraded areas are gradually decreasing (Figure 3). Regarding the spatial pattern, the Han River Basin exhibits a distribution pattern of "decrease-increase-decrease" from southeast to northwest. The significance test of the β value reveals that the areas with extremely significant and significant increases mainly lie in the central and northern parts of the basin. Conversely, the significant and extremely significant decrease in areas exhibits a "surrounding points" characteristic, predominantly concentrated in urban and riverside areas. The spatial distribution of vegetation *NDVI* in different geomorphic regions was analyzed through the combination of Theil–Sen trend analysis and Mann–Kendall significance values, resulting in the identification of distinct patterns (Figure 4). Regions displaying significant increases in vegetation cover are primarily found in low-relief mountains, medium undulating mountains, and hilly areas, encompassing mainly forest land, grass-shrub vegetation, or forest protection areas, which are significant sites for ecological protection and restoration efforts. Conversely, the areas experiencing extremely significant reductions are concentrated in plains and hilly regions. This decline in vegetation can be attributed to urban expansion encroaching on cultivated and forested lands, leading to their conversion into construction areas.

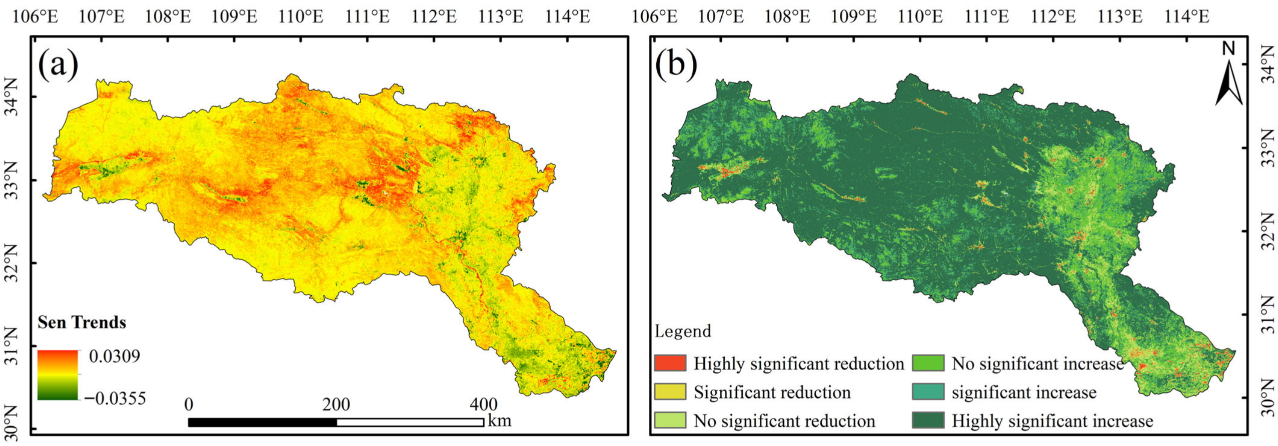

Figure 3. (**a**) The normalized difference vegetation index trend from 2000 to 2020.; (**b**) The significance test during the growing season from 2000 to 2020.

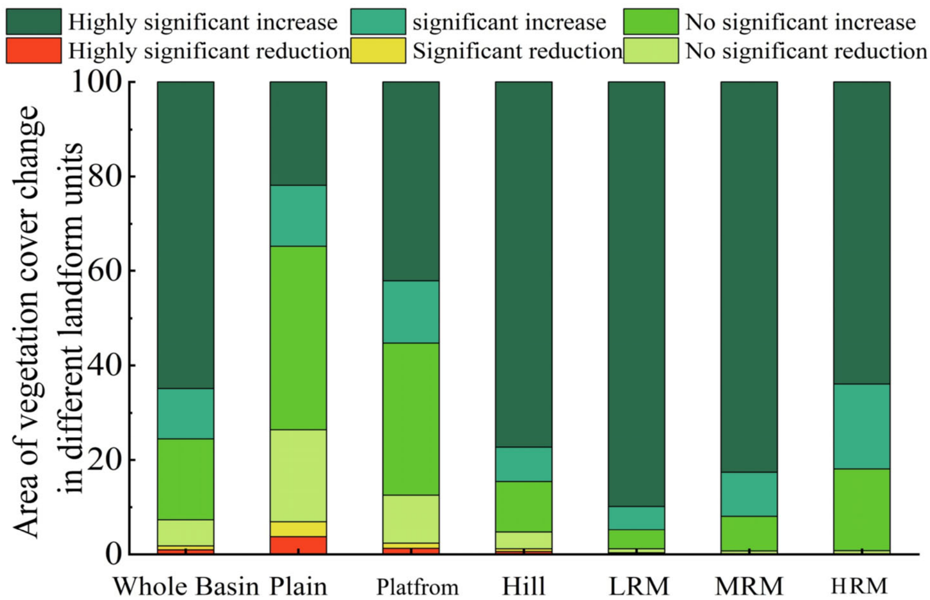

Figure 4. The normalized difference vegetation index variation trend of the growing season in different geomorphic regions.

3.3. Sustainability Characteristics of Vegetation Cover Change

The Hurst index of vegetation NDVI in the Han River Basin exhibited a range from 0.0814 to 0.9543 over the period of 2000 to 2020, with an average value of 0.5331. Notably, the proportion of the Hurst index greater than 0.5 in the Han River Basin is 65.80%, while the proportion of the Hurst index less than 0.5 is 34.20%. This indicates that the positive persistence of vegetation changes in the Han River Basin from 2000 to 2020 is stronger than the negative persistence (Figure 5). To elucidate the trend and sustainability of vegetation changes, NDVI trend change results were overlaid with the Hurst index outcomes. This overlay resulted in five distinct levels: continuous improvement, transition from increase to decrease, continuous degradation, transition from decrease to increase, and random change. The sustainable improvement of vegetation in the Han River Basin from 2000 to 2020 amounted to 31.16% of the total area.

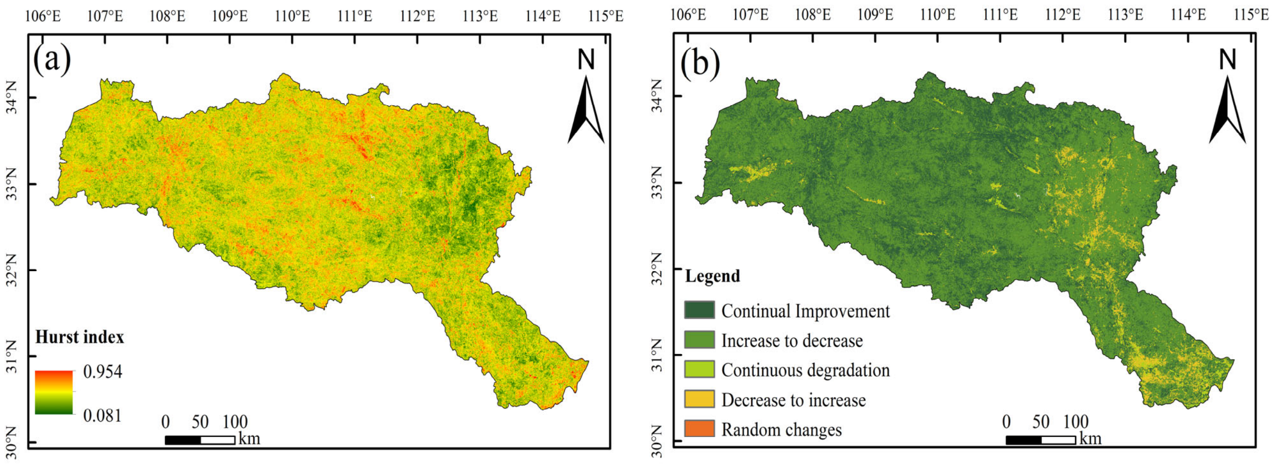

Figure 5. (**a**) the hurst index; (**b**) the normalized difference vegetation index trend in the growing season of the from 2000 to 2020.

This improvement was primarily concentrated in the central region of the basin. Additionally, there was a fluctuation of 61.50% in vegetation cover, with notable increases and decreases observed, particularly in the central and northwest areas of the basin. Continued degradation affected 4.28% of the area, predominantly concentrated along both sides of the main branches and tributaries of the Han River, forming a distinct strip-like distribution. A further 3.05% of the area exhibited a transition from decrease to increase in vegetation cover. It is imperative to maintain vigilance and redouble restoration efforts in areas experiencing continued degradation as well as those undergoing transitions from increase to decrease.

To understand the future change trend of vegetation *NDVI* in different geomorphic regions, it is essential to analyze the statistics on the future development trend of vegetation *NDVI* in each geomorphic type, which will enhance our comprehension of the structural patterns of future vegetation *NDVI* changes (Figure 6). The analysis indicates that in the future, the area of *NDVI* in the vegetation growth season across the watershed will shift from increasing to decreasing, with this trend predominating in each landform division. This implies that the future vegetation in different landform areas may transition from an increasing trajectory to a degrading direction.

In recent years, the significant recovery of vegetation *NDVI* in the Han River Basin has been largely attributed to the implementation of ecological restoration projects. However, considering the concept of diminishing marginal utility, the rapid restoration of vegetation might also escalate the complexity of restoring the remaining ecology to a certain extent. Notably, areas that exhibit continuous *NDVI* increase are primarily concentrated in low-relief mountains, medium-relief mountains, and hilly regions, which have been the focal points of recent ecological governance efforts. On the other hand, areas experiencing a shift from decreasing to increasing *NDVI* are mainly found in plains, platforms, and hilly areas, potentially linked to the development of diverse ecological restoration initiatives, such as the Yangtze River water supply project and the Han River shelterbelt project. Conversely, areas characterized by continuous reduction in *NDVI* are distributed in plains, platforms, and hilly regions situated within the economic development zone. These regions display a consistent downward trend in vegetation coverage *NDVI*. Notably, the areas along the Han River and the surrounding regions of the Wuhan urban agglomeration in the lower reaches require special attention, emphasizing the importance of prioritizing key ecological projects in these areas.

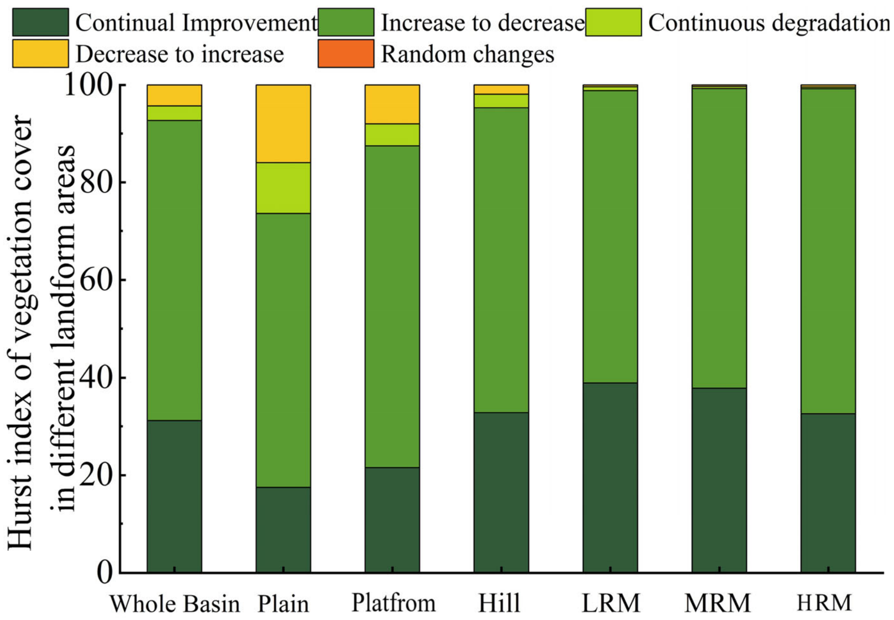

Figure 6. The normalized difference vegetation index trend of the growing season in the Han River Basin and different geomorphic regions from 2000 to 2020.

3.4. Vegetation NDVI and Climate Variability Trends and Their Correlations from 2000 to 2020

Climatic factors are the main natural factors controlling vegetation growth, with precipitation, temperature, solar radiation, relative humidity, and wind speed exerting significant influences on vegetation *NDVI*. Figure 7 shows the spatial distribution of climate fluctuations and climate change trends from 2000 to 2020. Over the past 20 years, warming and wetting trends are evident. From 2000 to 2020, precipitation, temperature, relative humidity, and annual average wind speed showed a slight upward trend, with the rate of change being 0.007 mm/a, 0.017 °C/a, 0.020%/a and 0.004 m/s/a, and the total solar radiation was −1.972 MJ/a (Figure 7a–e). During this period, temperatures rose in most areas of the Han River Basin, while slight drops were observed in the southwest and northeast regions. The variation in precipitation displayed a spatial difference opposite to that of air temperature. More specifically, regions experiencing higher temperatures often saw lower precipitation levels, and vice versa. The relative humidity showed a downward trend in the Nanyang Basin in the northeast, whereas it increased in other areas. Moreover, the overall wind speed exhibited an upward trend, while the northern and southern parts of the basin experienced a downward trend in wind speed.

The spatiotemporal trends in climatic factors provide valuable insights into the interactions between climate and vegetation dynamics in the Han River Basin. Understanding these patterns is crucial for formulating effective environmental management and conservation strategies to address the challenges posed by climate change and its impact on vegetation growth in the region.

To comprehend the response mechanisms of vegetation *NDVI* to climate change in the Han River Basin, we conducted an analysis of the correlation between vegetation *NDVI* and various climatic factors, including temperature, precipitation, total radiation, relative humidity, and average wind speed at the grid scale of the basin during the period from 2000 to 2020. Figure 8 illustrates the spatial distribution of correlation coefficients between *NDVI* and the aforementioned climatic variables. The findings revealed that within the Han River Basin, there were areas with both positive and negative correlations with precipitation, accounting for 55.89% and 44.11% of the total study area, respectively. In particular, the regions displaying positive correlations with precipitation were mainly concentrated in platform, hill, and plain areas. However, in HRM, precipitation exhibited a negative correlation with vegetation growth, indicating that the topography significantly influences vegetation development. Moreover, the Han River Basin exhibited positive and negative correlations with temperature, encompassing 70.65% and 19.35% of the total study area, respectively. Vegetation *NDVI* in landform units such as hills, and low-medium, and high-relief mountains demonstrated a positive correlation with temperature. As the fluctuation degree increased, the temperature sensitivity decreased and intensified, making heat the main limiting factor for vegetation growth. Conversely, plains and platforms displayed a negative correlation with temperature. Regarding total solar radiation, approximately 66.49% of the study area exhibited a positive correlation, while 33.51% displayed a negative correlation. Generally, sufficient precipitation supported vegetation growth, but excessive precipitation increased cloud cover, leading to reduced solar radiation and hampering the photosynthetic benefits of plants, thus adversely impacting vegetation growth [71]. These results provide crucial insights into the intricate relationship between climate factors and vegetation *NDVI* in the Han River Basin. Understanding such correlations is vital for devising effective climate-sensitive strategies for the sustainable management and conservation of the region's vegetation and ecosystem (Figure 9).

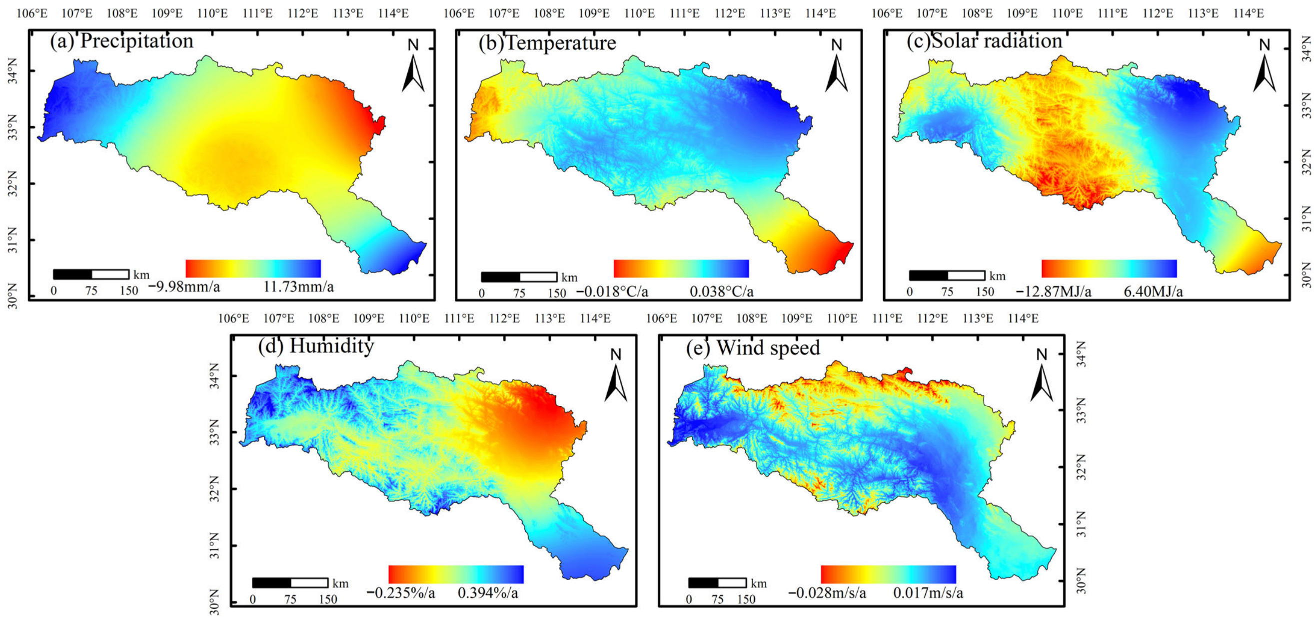

Figure 7. Spatial distribution of climate factors changes trends from 2000 to 2020.

From the perspective of the correlation between vegetation *NDVI* and relative humidity, approximately 66.49% of the areas exhibit positive correlations, while 33.51% show negative correlations. This indicates that relative humidity positively impacts the growth of vegetation *NDVI* in the Han River Basin, with the negative correlation areas primarily distributed at the edge of the Nanyang Basin and Han River valley. Notably, in landform units such as plains and hills, the negative correlation between vegetation *NDVI* and relative humidity is particularly strong. The lower annual precipitation in these areas results in reduced relative air humidity, limiting the water available for plant growth and thus constraining vegetation development. Regarding the correlation between annual mean wind speed and vegetation *NDVI*, the proportion of positive correlation (51.50%) is slightly higher than the proportion of negative correlation (48.50%). Areas where wind speed and vegetation *NDVI* display a negative correlation are primarily located in the northern and eastern parts of the Han River Basin. In landform units such as plains and platforms, vegetation *NDVI* exhibits a negative correlation with wind speed, with the strength of the negative correlation gradually decreasing. However, in hills, and low, medium and high-relief mountains, vegetation *NDVI* demonstrates a positive correlation with wind speed, with the highest positive correlation being observed in medium undulating mountains. Understanding the relationships between vegetation *NDVI* and climatic factors, such as relative humidity and wind speed, provides crucial insights into the complex interplay between climate and vegetation dynamics in the Han River Basin. These findings offer valuable guidance for developing targeted management strategies to enhance vegetation growth and ecological resilience in different regions of the basin.

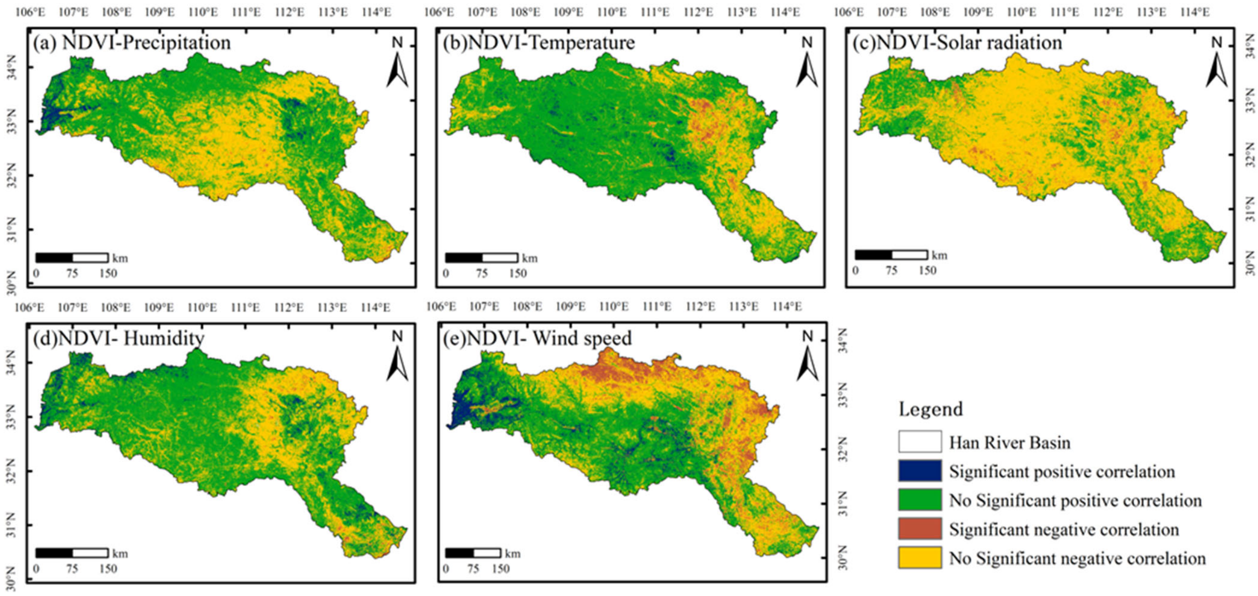

Figure 8. Correlation analysis of climatic factors and vegetation *NDVI* in the Han River Basin from 2000 to 2020.

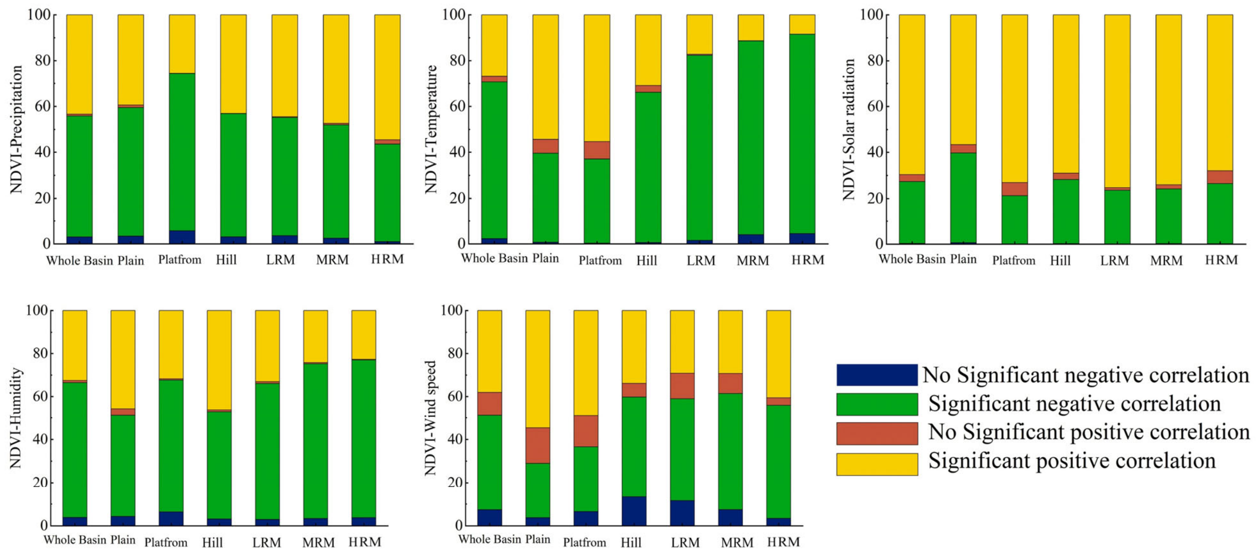

Figure 9. Significant correlation area between climate factors and vegetation *NDVI* in the Han River Basin and different geomorphic divisions.

3.5. Responses of Vegetation NDVI to Climate Change and Human Activities in the Han River Basin

Vegetation coverage changes are influenced not only by climatic factors but also by various human activities. To delve deeper into the relationship between vegetation coverage and human activities, this study employs the residual trend method to quantitatively analyze their impact on vegetation dynamics. From 2000 to 2020, the Han River Basin witnessed a substantial increase in vegetation coverage, accounting for a significant proportion of 92.18%, whereas the proportion of vegetation degradation was relatively small, at 7.82%

(Figure 10). Spatial analysis reveals that the degraded areas are mainly concentrated in the Wuhan urban agglomeration, while scattered occurrences are observed in the Nanyang Basin and along the river. The intertwined distribution of areas affected by climate change and human activities indicates that vegetation degradation is not the dominant mode of vegetation dynamics in the Han River Basin. The joint impact of climate change and human activities contributed to a substantial growth in vegetation coverage, accounting for 75.42%, with human activities alone driving 16.22% of vegetation growth, and climate change contributing a minor 0.54% (Figure 11). This suggests that *NDVI* vegetation recovery in the Han River Basin is primarily influenced by climate change and human activities. Notably, in the Nanyang Basin, vegetation growth driven by human activities in *NDVI* is particularly prominent, while other areas show scattered distribution, mainly in the southeast and northwest of the basin.

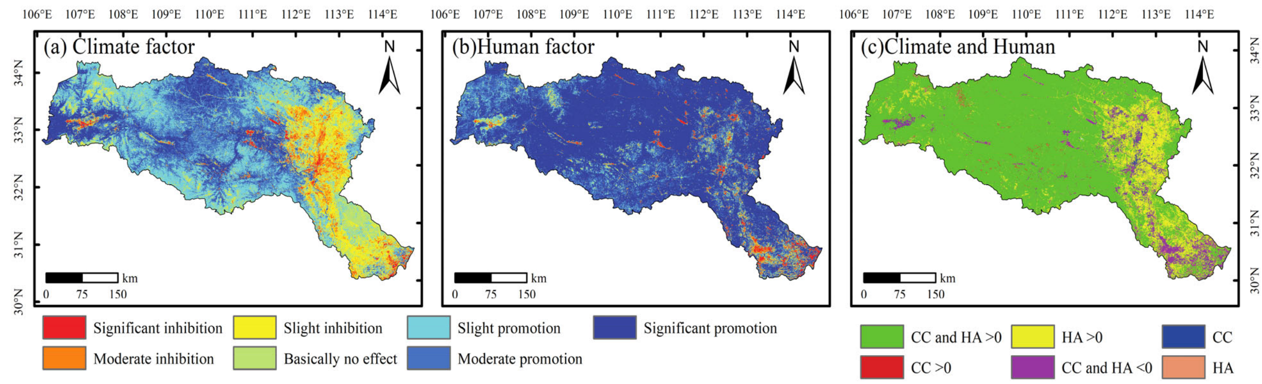

Figure 10. Spatial distribution of impacts of climate change and human activities on vegetation cover change from 2000 to 2020.

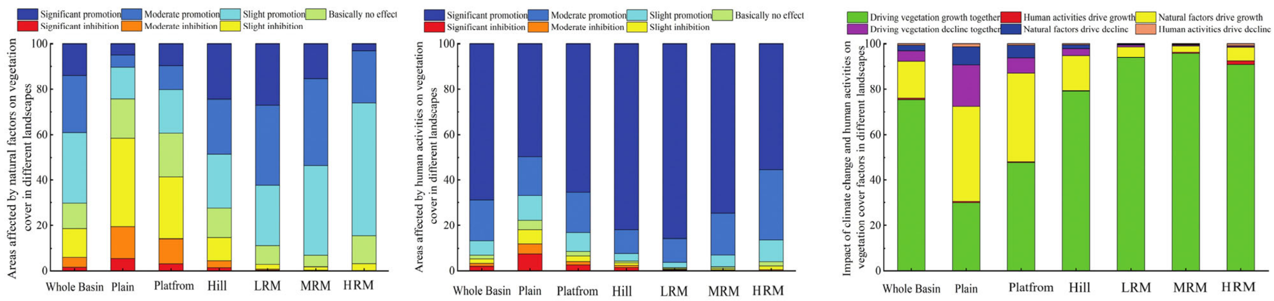

Figure 11. Percentage (%) of vegetation cover change due to climate change and human activities from 2000 to 2020.

Moreover, the influence of climate change and human activities on vegetation *NDVI* changes varies significantly across different geomorphological divisions, with plain areas experiencing different driving factors than other regions (Table 3). In plains, platforms, and hills, human activities predominantly suppress vegetation *NDVI*, whereas they promote vegetation growth in different mountainous landforms. Overall, human activities have a greater contribution to the increase in *NDVI* changes than climate change in most parts of the Han River Basin. The impact of human activities on *NDVI* changes is particularly notable in the plains, platforms, and hills, accounting for 49.05%, 39.01%, and 15.54%, respectively. In mountainous areas, both natural and human activities have a combined effect, exceeding 90% in influencing vegetation dynamics.

Table 3. Driving art criterion and contribution rate calculation method of vegetation *NDVI* change.

Slope ($NDVI_{OBS}$) [a]	Driving Factor	Classification Criteria		Contribution Rate (%)	
		$Slope(NDVI_{CC})$ [b]	$Slope(NDVI_{HA})$ [c]	Climate Change (*CC*)	Human Activity (*HA*)
>0	*CC* and *HA*	>0	>0	$\frac{slope(NDVI_{CC})}{slope(NDVI_{obs})}$	$\frac{slope(NDVI_{CC})}{slope(NDVI_{obs})}$
	CC	>0	<0	100	0
	HA	<0	>0	0	100
<0	*CC* and *HA*	<0	<0	$\frac{slope(NDVI_{CC})}{slope(NDVI_{obs})}$	$\frac{slope(NDVI_{CC})}{slope(NDVI_{obs})}$
	CC	<0	>0	100	0
	HA	>0	<0	0	100

"a", "b" and "c" have no specific meaning or numerical value. The purpose is to differentiate between actual values, predicted values, and residual values.

In summary, the Han River Basin experiences significant vegetation dynamics, where human activities play a substantial role in driving positive changes in vegetation coverage, along with climate change. The impact of these factors varies across different regions and geomorphological divisions, emphasizing the need for targeted management strategies to ensure sustainable vegetation and ecosystem management in the region.

3.6. Relative Contributions of Climate Change and Human Activities to Vegetation NDVI Changes in the Han River Basin

Figure 12 illustrates the spatial distribution of the contribution rate of vegetation *NDVI* change in the Han River Basin from 2000 to 2020. It is evident from the figure that climate change plays a relatively minor role in improving the area of vegetation *NDVI*, accounting for only 25.41%. The contribution rate of climate change to the improvement in vegetation *NDVI* is predominantly concentrated in the range of 0–20%, with only a small portion (0.56%) falling in the 80–100% range, primarily scattered in the south-central and northwest regions of the Han River Basin. In contrast, human activities take the lead in driving the improvement in vegetation *NDVI* in the Han River Basin, accounting for 74.59% of the contribution rate. The areas with a contribution rate of more than 80% cover 23.98% of the vegetation improvement area, mainly distributed in the eastern part of the Han River Basin, the Nanyang Basin, and the lower reaches.

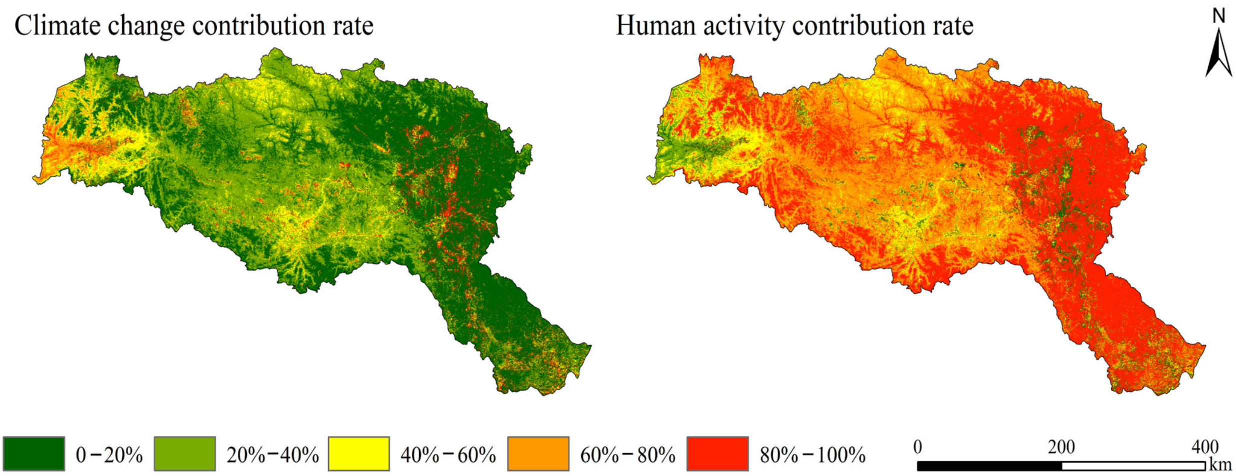

Figure 12. Spatial distribution of contribution rates of climate change and human activities to vegetation cover change in the Han River Basin.

Regarding the vegetation degraded area, the contribution rate of climate change to vegetation change is higher compared to the vegetation improvement area and also surpasses the effect of human activities. In this case, the contribution rate of climate change to vegetation *NDVI* degradation is relatively significant in the 80–100% range, accounting for 19.67% of the vegetation degraded area, mainly distributed in the southeast of the Han River Basin and other regions. Additionally, the contribution of human activities to vegetation *NDVI* degradation is also relatively notable, with the area featuring a contribution rate of more than 80% accounting for 9.29% of the vegetation degraded area, primarily located in the lower reaches of the Han River and the Nanyang Basin. The contrasting roles of climate change and human activities in vegetation dynamics warrant careful consideration for sustainable land management and conservation efforts in the Han River Basin.

In various landform divisions of the Han River Basin, human activities played a significant role in enhancing the *NDVI* in the vegetation improvement area. Particularly, in the plain area, human activities accounted for the highest contribution, reaching 90.28%. This trend was also observed in platforms, hills, low-relief mountains, high-relief mountains, and medium relief mountains, with human activities contributing over 70% to *NDVI* improvement. Conversely, in areas where vegetation *NDVI* degraded, climate change had notable contributions to degradation in plains, platforms, hills, and low-relief mountains, with contribution rates of 59.08%, 70.90%, 62.16%, and 52.61% (Figure 13), respectively. Notably, during the degradation of vegetation *NDVI* in medium and high-relief mountains, human activities played a more dominant role, with contribution rates of 58.61% and 72.12%, respectively. The intricate interplay between human activities and climate change in different landform regions highlights the necessity for targeted management strategies to ensure sustainable vegetation and ecosystem management in the Han River Basin.

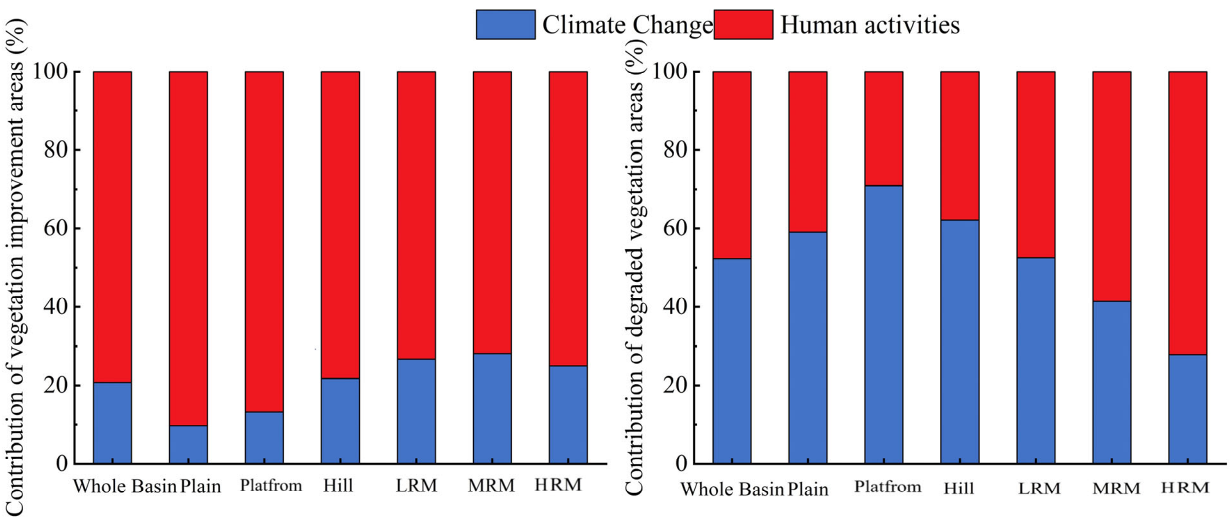

Figure 13. Relative contributions of climate change and human activities to *NDVI* changes in the Han River Basin and different geomorphic regions.

4. Discussion

4.1. Temporal and Spatial Evolution Characteristics of Vegetation NDVI in the Study Area

From 2000 to 2020, the *NDVI* of the vegetation in the Han River Basin exhibited an overall fluctuating upward trend. However, distinct spatiotemporal heterogeneity was observed across different geomorphic units, aligning with previous research findings [49,51]. The *NDVI* peaks in the Han River Basin occurred in 2001 and 2015, respectively, with subsequent years showing continuous *NDVI* increases, while the lowest value appeared in 2001, largely attributed to abnormal drought conditions in the basin.

Notably, various ecological projects have been implemented in the Han River Basin since 2000, such as the Shelterbelt Project, Natural Forest Protection Project, and Project of Returning Farmland to Forest and Grassland [47]. These initiatives significantly increased woodland and grassland areas in low-relief mountains and hilly regions, leading to an overall upward trend in vegetation coverage, particularly higher than that in medium and high-relief mountain areas. Conversely, vegetation degradation was evident in plain and platform regions, mainly driven by rapid urbanization processes. The conversion of substantial amounts of cultivated and forest land into construction land contributed to the downward trend of vegetation *NDVI* in the Wuhan urban agglomeration and surrounding areas, corroborating existing research [72–74]. After 2016, the growth of vegetation *NDVI* in the Han River Basin was relatively stable, and the fluctuations were small. With the establishment of the ecological strategy of "jointly grasping great protection and not engaging in large-scale development" in the Yangtze River Basin, and the large-scale implementation of returning farmland to forests and lakes in the watershed ecological protection and construction projects such as water and soil conservation have gradually highlighted ecological benefits.

4.2. Effects of Climate Change and Human Activities on Vegetation NDVI Dynamics in the Han River Basin

The Han River Basin, a significant ecological barrier area, exemplifies the intricate interplay between topography, climate, and human activities. Various geomorphic types within the basin possess distinct mechanisms of influence on hydrothermal conditions. The appropriate combination of these conditions can enhance vegetation growth, while an unsuitable combination may hinder it. Notably, the temporal and spatial evolution of vegetation *NDVI* during the growing season is influenced not only by temperature and precipitation but also by other climatic factors such as sunshine and humidity [34,35,74]. This study goes beyond previous research, which mainly focused on the response mechanism of precipitation and temperature to vegetation *NDVI* [69,73,74]. Instead, it incorporates additional meteorological factors, including total solar radiation, relative humidity, and annual average wind speed, to investigate the correlation between climate factors and *NDVI*. By doing so, this research offers a comprehensive depiction of the response of vegetation *NDVI* to meteorological factors.

The correlation analysis reveals that temperature exerts a more substantial impact on vegetation *NDVI* than precipitation, relative humidity, average wind speed, and total solar radiation. This observation highlights the significant influence of water and heat conditions on vegetation growth. Furthermore, distinct climatic factors exhibit diverse mechanisms of action on vegetation growth, and the effects of the same climatic factor may vary across different regions. Over the past 21 years, the Han River Basin has experienced a gradual increase in overall precipitation, temperature, relative humidity, and annual average wind speed.

This research advances our understanding of the intricate relationships between climate factors and vegetation dynamics in the Han River Basin. By considering a broader range of meteorological factors, it contributes to a more comprehensive assessment of the drivers behind vegetation changes. The findings hold valuable implications for environmental management and conservation efforts aimed at mitigating the impacts of climate change and optimizing vegetation growth in the region.

The observed trends in the Han River Basin's vegetation dynamics are consistent with regional climate changes, which have been shifting towards warmer and more humid conditions [75]. Climatic warming and increased humidity have rendered higher altitude areas more susceptible to climate change [76]. Simultaneously, they have alleviated the constraints of low temperatures and drought on high-altitude vegetation growth, leading to extended vegetation growth periods and promoting overall vegetation growth [77]. In areas with higher relief, such as mountainous regions, the temperature decline caused by adequate precipitation becomes a significant limiting factor for vegetation growth [78]. Conversely, in platform and plain areas, where precipitation is relatively lower and temperatures higher, the heat conditions required for vegetation growth are more favorable. Optimal wind speeds can promote plant growth and increase vegetation coverage, but strong or sustained winds can damage plants and hinder vegetation growth [79]. The highest vegetation coverage is observed in medium undulating mountains, effectively mitigating the adverse impact of excessive wind speeds on vegetation growth. Conversely, in landform units like low-relief mountains, hills, platforms, and plains, where relief is lower, vegetation coverage demonstrates a downward trend, with increasing wind speeds inhibiting vegetation *NDVI* growth. In summary, the spatiotemporal dynamics of vegetation in the Han River Basin are strongly influenced by various climatic factors. Understanding these relationships is essential for implementing effective measures to manage and conserve the region's ecosystems, considering the differential effects of climate change and natural topographic variations on vegetation growth.

Elevated temperatures beyond the optimum range weaken the net photosynthesis of vegetation, increase evaporation, and exacerbate water scarcity [80]. Consequently, increased temperatures hinder the growth of *NDVI* in landform units like platforms and plains. The *NDVI* of vegetation in the Han River Basin and different geomorphic units exhibits a negative correlation with total solar radiation, consistent with prior research [52]. As a humid region, the Han River Basin generally receives sufficient precipitation to meet vegetation's growth requirements. However, excessive precipitation can lead to increased cloud cover, reducing solar radiation, diminishing photosynthetic benefits, and adversely impacting vegetation growth. Relative humidity, on the other hand, promotes the growth of vegetation *NDVI* in the Han River Basin, while low annual precipitation in landform units like plains and hills results in decreased air humidity, limiting vegetation growth due to reduced water availability. Optimal wind speeds can promote plant growth and increase vegetation coverage, but strong or sustained winds can damage plants and hinder vegetation growth [79].

The highest vegetation coverage is observed in medium undulating mountains, effectively mitigating the adverse impacts of excessive wind speeds on vegetation growth. Conversely, in landform units like low-relief mountains, hills, platforms, and plains, where relief is lower, vegetation coverage demonstrates a downward trend, with increasing wind speeds inhibiting vegetation *NDVI* growth. In summary, the spatiotemporal dynamics of vegetation in the Han River Basin are strongly influenced by various climatic factors. Understanding these relationships is essential for implementing effective measures to manage and conserve the region's ecosystems, considering the differential effects of climate change and natural topographic variations on vegetation growth.

Based on the residual analysis results (Figure 10), it is evident that human activities, in addition to climate change, play a crucial role in shaping the spatial distribution pattern and dynamic changes of vegetation, particularly in plains and platforms within the Han River Basin. Human-induced factors have a significant impact on the increase in *NDVI*, with their influence concentrated in areas like the Nanyang Basin and Jianghan Plain. These regions, characterized by extensive agricultural land cover, demonstrate enhanced vegetation growth, largely attributed to modern science and technology advancements supporting crop production [80]. On the other hand, both climate change and human activities can contribute to the inhibition of vegetation coverage growth, leading to a noticeable degradation trend in vegetation *NDVI* across the basin (Figure 10). Notably, landform units such as plains and platforms experience negative impacts on vegetation *NDVI* changes due to factors like decreased precipitation, relative humidity, and increased air temperature and total solar radiation since 2000. The drier climate conditions in these areas, coupled with rapid warming, may exacerbate water shortages and subsequently limit vegetation growth [63]. In specific locations like the Wuhan urban agglomeration and certain cities (Figure 4), the negative impact of human activities on vegetation changes is more pronounced, primarily due to urbanization encroaching upon farmland and forested areas. Therefore, in the context of food security, it is crucial to address the adverse effects of human activities on crop growth.

This study highlights that vegetation restoration efforts in the Han River Basin, across different landform units, are significantly influenced by human activities, contributing more than 70% to the increase in vegetation *NDVI* during the growing season from 2000 to 2020. In comparison, in areas experiencing vegetation degradation, climate change plays a more substantial role than human activities. The interplay of climate change and human-induced factors holds decisive significance in shaping the spatial distribution of vegetation *NDVI* changes within the Han River Basin. Government-led ecological protection projects, such as returning farmland to the forest (grass) and natural forest protection, have been pivotal drivers of the increase in vegetation coverage [47,52]. Overall, understanding the intricate relationships between climate change, human activities, and vegetation dynamics is crucial for effective ecological management and conservation strategies in the Han River Basin, contributing to the broader goal of sustainable development in the region.

4.3. Data innovation for Quantitative Analysis of Vegetation Changes and Human Activities

Vegetation change and quantitative analysis of human activities have made significant progress in data innovation for data acquisition. In this study, we utilized the MOD13Q1 NDVI dataset. However, with the continuous advancement of technology, remote sensing and aerospace technology have provided us with more satellite resources for land use monitoring. A noteworthy example is the "Sustainable Development Scientific Satellite 1" (SDGSAT-1) launched by China in 2022. It is the world's first scientific satellite dedicated to serving the United Nations' 2030 Agenda for Sustainable Development. The satellite aims to detect surface parameters closely related to human activities, finely monitor the interaction between human activities and the natural environment, accurately detect changes in water quality in different water bodies [81,82], and assess economic and social indices for precise evaluation of human settlements [16,83,84]. It provides high-quality data support for global sustainable development goal monitoring, evaluation, and scientific research by offering dynamic, multiscale, and periodic information. Additionally, the application of artificial intelligence and machine learning techniques in the data processing process enables efficient, in-depth, and comprehensive quantitative analysis of large-scale remote sensing data [85,86]. The use of these technologies will provide us with more precise data, allowing us to gain a more accurate understanding of the relationship between vegetation changes and human activities, thus providing stronger support for sustainable development.

4.4. Models That Account for the Complex Interactions between Climate, Human Activities, and Vegetation

The response mechanism of vegetation to climate change and human activities is a complex and multifaceted process, influenced by various interconnected factors. Beyond the mentioned climatic factors, other variables such as evapotranspiration and soil moisture also play significant roles in affecting vegetation *NDVI*. Moreover, research on the lag effect of vegetation response to climate change remains a critical aspect that requires further investigation.

In future studies, it is essential to develop a more comprehensive and sophisticated model that considers the intricate interplay between climate change, human activities, and vegetation dynamics. This model should not only take into account the direct impacts of these factors but also consider their lag effects and interactions with other relevant variables. Quantifying the precise and detailed influence of different human activities on vegetation *NDVI* poses a significant challenge, and addressing this challenge will be crucial for enhancing our understanding of the complex relationship between human-induced changes and vegetation response [87]. By refining and expanding the current research approaches, a more comprehensive understanding of vegetation dynamics in response to climate change and human activities can be attained. This knowledge is essential for guiding effective environmental management, conservation strategies, and sustainable development practices, ultimately contributing to the ecological stability and balance in the Han River Basin and similar regions.

5. Conclusions

This study conducted an analysis of the spatial-temporal distribution and changing trends of vegetation within the Han River Basin from 2000 to 2020, with a focus on *NDVI*. Various landform zoning perspectives were employed for this analysis. Analytical tools such as Theil–Sen trend analysis, Mann–Kendall significance test, Hurst index, and correlation were utilized to achieve this. The multiple regression residual analysis method was primarily employed in this study to conduct a preliminary analysis of the impact of climate change and human activities on vegetation *NDVI* in the Han River Basin. This comprehensive approach provided a deeper understanding of the factors influencing vegetation dynamics in the Han River Basin during the study period. It is worth noting that this study addressed these issues at the level of mathematical statistics. Further research is essential to elucidate the underlying mechanisms and variations in the influence of different periods. Therefore, forthcoming studies should consider a broader spectrum of factors. These may include climate parameters (such as sunshine hours, radiation, relative humidity, etc.), human activity data (urbanization, LUCC, etc.), and vegetation changes (NPP, EVI, etc.). Additionally, employing more efficient methods will enable a more comprehensive exploration of the impacts of climate change and human activities on vegetation dynamics.

(1) Between 2000 and 2020, the *NDVI* for vegetation in the Han River Basin exhibited a consistent and overall increasing trend across various landform units. However, the extent of *NDVI* growth varied due to the distinct sensitivity and characteristics of the local natural environment. Notably, the most significant increase in *NDVI* was observed in low-relief mountain regions, demonstrating the heightened responsiveness of vegetation in these areas. On the other hand, the plain and platform vegetation exhibited lower growth rates, specifically at 1.56% per decade and 2.93% per decade, respectively. These values were below the average growth rate of the entire basin, which stood at 3.78% per decade. These findings emphasize the differentiated responses of vegetation to changing conditions in different landform regions within the Han River Basin. Understanding such variations is essential for effective ecosystem management and conservation strategies in the region.

(2) In space, the distribution pattern of "decrease-increase-decrease" appears from southeast to northwest. Low-altitude hills, middle-altitude hills, and low-relief mountains show a greening trend with a larger percentage of vegetation. Of these, low-relief mountains showed the best improvement in vegetation, and plains vegetation showed the largest proportion of degrading trends, mainly with no significant downward trend, comprising 19.54% of the total area.

(3) Upon analyzing the response of vegetation to climate factors, it is evident that the spatial distribution of *NDVI* in the region exhibits positive correlations with precipitation, temperature, relative humidity, and average wind speed. Conversely, it demonstrates a negative correlation with total solar radiation. Notably, the impact of temperature on vegetation *NDVI* outweighs that of other meteorological factors, signifying its greater significance in shaping vegetation patterns. Furthermore, the response of vegetation *NDVI* to climatic factors vary across different geomorphic units within the watershed. Specifically, in plains, platforms, and similar geomorphic units, there is a significant negative correlation observed between vegetation *NDVI* and air temperature, as well as average wind speed. In contrast, in hilly terrain, low-relief mountains, and middle areas such as undulating mountains, a significant positive correlation between vegetation *NDVI* and these climatic factors is evident ($p < 0.05$). These findings emphasize the importance of considering the diverse geomorphic characteristics of the region while understanding the complex interplay between vegetation and climate factors. The positive correlation observed in certain areas may be indicative of favorable conditions for vegetation growth, while the negative correlation in other regions may signal potential stress on vegetation due to climatic factors.

(4) The impact of both climate change and human activities on vegetation *NDVI* changes in the Han River Basin exhibits significant spatial heterogeneity, predominantly manifesting as a promotion of vegetation growth. Notably, the influence of human activities on vegetation *NDVI* changes outweighs that of climate change, indicating a more potent effect. In the context of degradation, areas where vegetation *NDVI* changes are driven by both climate and human activities, accounted for 4.77% of the total,

with climate-related factors contributing to 2.46% and human activities accounting for 2.31%. On the other hand, areas influenced solely by climate factors accounted for 0.54%, while those solely driven by human activities constituted a more substantial proportion of 16.22%. A noteworthy observation is that the regions where vegetation *NDVI* improvement was primarily driven by human activities were predominantly distributed across various landform units, including plains, platforms, and hills. These findings underscore the complex interplay between climate change and human activities in shaping vegetation dynamics within the Han River Basin. Moreover, they highlight the dominant role of human activities in promoting vegetation growth and indicate the necessity for targeted management strategies that consider both climate change and human-induced impacts to ensure sustainable vegetation and ecosystem management in the region.

(5) In recent years, the alterations in vegetation *NDVI* within the Han River Basin have been primarily influenced by a combination of climate change and human activities. Over the past two decades, climate change and human activities have contributed to these changes at relative rates of 25.41% and 74.59%, respectively. Specifically, when considering the vegetation improvement area of the Han River Basin, the respective contributions of climate change and human activities to *NDVI* changes were 25.41% and 74.59%. Conversely, in the vegetation degradation area, their contributions were 59.77% and 40.23%, respectively. These findings highlight that human activities play a decisive role in shaping vegetation coverage in the Han River Basin. Considering the implications for future vegetation protection and management, it is imperative to not only acknowledge the positive impact of human activities, but also to address the potential interference of climate change. Consequently, a comprehensive approach must be adopted to sustainably manage the vegetation and ecosystem in the Han River Basin.

Author Contributions: Conceptualization, Y.X. and Z.Z.; methodology, Y.X.; software, Y.X. and Z.Z.; validation, S.L.; formal analysis, Z.Z.; investigation, C.W.; resources, L.W. (Li Wang); data curation, Y.X.; writing—original draft preparation, Y.X. and Z.Z.; writing—review and editing, L.W. (Lei Wang) and M.F.; visualization, Z.Z.; supervision, L.W. (Lei Wang); project administration, M.F.; funding acquisition, L.W. (Lei Wang). All authors have read and agreed to the published version of the manuscript.

Funding: This research was supported by the National Key Research and Development Program of China (grant number 2022YFC3800700) and the Youth Innovation Promotion Association, CAS (grant number 2022122).

Data Availability Statement: Data is contained within the article.

Acknowledgments: The authors would like to thank editors and reviewers for their constructive comments and suggestions.

Conflicts of Interest: The authors declare no conflict of interest.

References

1. Derakhshannia, M.; Dalvand, S.; Asakereh, B.; Askari, K. Corrosion and deposition in Karoon River, Iran, based on hydrometric stations. *Int. J. Hydrol. Sci. Technol.* **2020**, *10*, 334. [CrossRef]
2. Zhang, Z.; Liu, H.; Zuo, Q.; Yu, J.; Li, Y. Spatiotemporal change of fractional vegetation cover in the Yellow River Basin during 2000–2019. *Resour. Sci.* **2021**, *43*, 849–858.
3. Hou, W.; Hou, X. Spatial-temporal changes in vegetation coverage in the global coastal zone based on GIMMS NDVI3g data. *Int. J. Remote Sens.* **2020**, *41*, 1118–1138. [CrossRef]
4. Chen, T.; Xia, J.; Zou, L.; Hong, S. Quantifying the Influences of Natural Factors and Human Activities on NDVI Changes in the Hanjiang River Basin, China. *Remote Sens.* **2020**, *12*, 3780. [CrossRef]
5. Li, Y.; Li, Z.; Zhang, X.; Gui, J.; Xue, J. Vegetation variations and its driving factors in the transition zone between Tibetan Plateau and arid region. *Ecol. Indic.* **2022**, *141*, 109101. [CrossRef]
6. Zhang, Y.; Jiang, X.; Lei, Y.; Gao, S. The contributions of natural and anthropogenic factors to NDVI variations on the Loess Plateau in China during 2000–2020. *Ecol. Indic.* **2022**, *143*, 109342. [CrossRef]

7. Liu, C.; Liu, J.; Zhang, Q.; Ci, H.; Gu, X.; Gulakhmadov, A. Attribution of NDVI Dynamics over the Globe from 1982 to 2015. *Remote Sens.* **2022**, *14*, 2706. [CrossRef]
8. Gu, Y.; Pang, B.; Qiao, X.; Xu, D.; Li, W.; Yan, Y.; Dou, H.; Ao, W.; Wang, W.; Zou, C.; et al. Vegetation dynamics in response to climate change and human activities in the Hulun Lake basin from 1981 to 2019. *Ecol. Indic.* **2022**, *136*, 108700. [CrossRef]
9. Liu, Y.; Zhao, W.; Hua, T.; Wang, S.; Fu, B. Slower vegetation greening faced faster social development on the landscape of the Belt and Road region. *Sci. Total Environ.* **2019**, *697*, 134103. [CrossRef]
10. Ma, M.; Wang, Q.; Liu, R.; Zhao, Y.; Zhang, D. Effects of climate change and human activities on vegetation coverage change in northern China considering extreme climate and time-lag and -accumulation effects. *Sci. Total Environ.* **2023**, *860*, 160527. [CrossRef]
11. Seddon, A.W.R.; Macias-Fauria, M.; Long, P.R.; Benz, D.; Willis, K.J. Sensitivity of global terrestrial ecosystems to climate variability. *Nature* **2016**, *531*, 229–232. [CrossRef] [PubMed]
12. Sun, Y.; Yi, L.; Yin, S. Vegetation Cover Change in Dongting Lake Basin and Its Coordination Governance. *Econ. Geogr.* **2022**, *42*, 190–201. [CrossRef]
13. Honeck, E.; Castello, R.; Chatenoux, B.; Richard, J.-P.; Lehmann, A.; Giuliani, G. From a Vegetation Index to a Sustainable Development Goal Indicator: Forest Trend Monitoring Using Three Decades of Earth Observations across Switzerland. *ISPRS Int. J. Geo-Inf.* **2018**, *7*, 455. [CrossRef]
14. Chen, F.; Wang, J.; Li, B.; Yang, A.; Zhang, M. Spatial variability in melting on Himalayan debris-covered glaciers from 2000 to 2013. *Remote Sens. Environ.* **2023**, *291*, 113560. [CrossRef]
15. Gao, J.; Zhang, Z.; Li, W.; Sun, F.; Hu, Y.; Wang, L.; Fu, J.; Li, X.; Cheng, G. Urban Sustainable Development Evaluation with Big Earth Data: Data, Indicators, and Methods. *Bull. Chin. Acad. Sci.* **2021**, *36*, 940–949. [CrossRef]
16. Li, C.; Chen, F.; Wang, N.; Yu, B.; Wang, L. SDGSAT-1 nighttime light data improve village-scale built-up delineation. *Remote Sens. Environ.* **2023**, *297*, 113764. [CrossRef]
17. Li, Y.; Xie, Z.; Qin, Y.; Zheng, Z. Estimating Relations of Vegetation, Climate Change, and Human Activity: A Case Study in the 400 mm Annual Precipitation Fluctuation Zone, China. *Remote Sens.* **2019**, *11*, 1159. [CrossRef]
18. Chen, F.; Wang, N.; Yu, B.; Wang, L. Res2-Unet, a New Deep Architecture for Building Detection from High Spatial Resolution Images. *IEEE J. Sel. Top. Appl. Earth Obs. Remote Sens.* **2022**, *15*, 1494–1501. [CrossRef]
19. Bai, Y.; Yang, Y.; Jiang, H. Intercomparison of AVHRR GIMMS3g, Terra MODIS, and SPOT-VGT NDVI Products over the Mongolian Plateau. *Remote Sens.* **2019**, *11*, 2030. [CrossRef]
20. Chen, T.; Xia, J.; Zou, L.; Yan, Q. Spatiotemporal variations of NDVI of different vegetation types in the Baiyangdian Basin under the background of climate change. *Resour. Sci.* **2021**, *43*, 1248–1259. [CrossRef]
21. Yin, G.; Hu, Z.; Chen, X.; Tiyip, T. Vegetation dynamics and its response to climate change in Central Asia. *J. Arid. Land* **2016**, *8*, 375–388. [CrossRef]
22. Li, M.; Du, J.; Li, W.; Li, R.; Wu, S.; Wang, S. Global Vegetation Change and Its Relationship with Precipitation and Temperature Based on GLASS-LAI in 1982–2015. *Sci. Geol. Sin.* **2020**, *40*, 823–832. [CrossRef]
23. Sun, Y.; Shan, M.; Pei, X.; Zhang, X.; Yang, Y. Assessment of the impacts of climate change and human activities on vegetation cover change in the Haihe River basin, China. *Phys. Chem. Earth* **2020**, *115*, 102834. [CrossRef]
24. Cheng, D.; Qi, G.; Song, J.; Zhang, Y.; Bai, H.; Gao, X. Quantitative Assessment of the Contributions of Climate Change and Human Activities to Vegetation Variation in the Qinling Mountains. *Front. Earth Sci.* **2021**, *9*, 7823. [CrossRef]
25. Nemani, R.R.; Keeling, C.D.; Hashimoto, H.; Jolly, W.M.; Piper, S.C.; Tucker, C.J.; Myneni, R.B.; Running, S.W. Climate-Driven Increases in Global Terrestrial Net Primary Production from 1982 to 1999. *Science* **2003**, *300*, 1560–1563. [CrossRef]
26. Ji, S.; Ren, S.; Li, Y.; Dong, J.; Wang, L.; Quan, Q.; Liu, J. Diverse responses of spring phenology to preseason drought and warming under different biomes in the North China Plain. *Sci. Total Environ.* **2021**, *766*, 144437. [CrossRef]
27. Zheng, K.; Wei, J.-Z.; Pei, J.-Y.; Cheng, H.; Zhang, X.-L.; Huang, F.-Q.; Li, F.-M.; Ye, J.-S. Impacts of climate change and human activities on grassland vegetation variation in the Chinese Loess Plateau. *Sci. Total Environ.* **2019**, *660*, 236–244. [CrossRef]
28. Zhou, X.; Yamaguchi, Y.; Arjasakusuma, S. Distinguishing the vegetation dynamics induced by anthropogenic factors using vegetation optical depth and AVHRR NDVI: A cross-border study on the Mongolian Plateau. *Sci. Total Environ.* **2018**, *616*, 730–743. [CrossRef]
29. Shi, S.; Yu, J.; Wang, F.; Wang, P.; Zhang, Y.; Jin, K. Quantitative contributions of climate change and human activities to vegetation changes over multiple time scales on the Loess Plateau. *Sci. Total Environ.* **2021**, *755*, 142419. [CrossRef]
30. Huang, S.; Zheng, X.; Ma, L.; Wang, H.; Huang, Q.; Leng, G.; Meng, E.; Guo, Y. Quantitative contribution of climate change and human activities to vegetation cover variations based on GA-SVM model. *J. Hydrol.* **2020**, *584*, 124687. [CrossRef]
31. Gu, L.; Gong, Z.; Du, Y. Evolution characteristics and simulation prediction of forest and grass landscape fragmentation based on the "Grain for Green" projects on the Loess Plateau, P.R. China. *Ecol. Indic.* **2021**, *131*, 108240. [CrossRef]
32. Ge, W.; Deng, L.; Wang, F.; Han, J. Quantifying the contributions of human activities and climate change to vegetation net primary productivity dynamics in China from 2001 to 2016. *Sci. Total Environ.* **2021**, *773*, 145648. [CrossRef] [PubMed]
33. John, R.; Chen, J.; Kim, Y.; Ou-yang, Z.-t.; Xiao, J.; Park, H.; Shao, C.; Zhang, Y.; Amarjargal, A.; Batkhshig, O.; et al. Differentiating anthropogenic modification and precipitation-driven change on vegetation productivity on the Mongolian Plateau. *Landsc. Ecol.* **2016**, *31*, 547–566. [CrossRef]

34. Emamian, A.; Rashki, A.; Kaskaoutis, D.G.; Gholami, A.; Opp, C.; Middleton, N. Assessing vegetation restoration potential under different land uses and climatic classes in northeast Iran. *Ecol. Indic.* **2021**, *122*, 107325. [CrossRef]
35. Wang, Y.; Dai, E.; Wu, C. Spatiotemporal heterogeneity of net primary productivity and response to climate change in the mountain regions of southwest China. *Ecol. Indic.* **2021**, *132*, 108273. [CrossRef]
36. Deng, C.; Bai, H.; Gao, S.; Liu, R.; Ma, X.; Huang, X.; Meng, Q. Spatial-temporal Variation of the Vegetation Coverage in Qinling Mountains and Its Dual Response to Climate Change and Human Activities. *J. Nat. Resour.* **2018**, *33*, 425–438. [CrossRef]
37. Zhang, M.; Wu, X. The rebound effects of recent vegetation restoration projects in Mu Us Sandy land of China. *Ecol. Indic.* **2020**, *113*, 106228. [CrossRef]
38. Xu, Y.; Zheng, Z.; Dai, Q.; Guo, Z.; Pan, Y. Attribution analysis of vegetation NPP variation in Southwest China considering time-lag effects. *Trans. Chin. Soc. Agric. Eng.* **2022**, *38*, 297–305+339. [CrossRef]
39. Yi, L.; Ren, Z.; Zhang, C.; Liu, W. Vegetation Cover, Climate and Human Activities on the Loess Plateau. *Resour. Sci.* **2014**, *36*, 166–174.
40. Guo, M.; Zhang, T.; Zhang, J.; Chen, L.; Zhang, X. Response of Vegetation Coverage to Climate Change in the Loess Plateau in 1982–2006. *Res. Soil Water Conserv.* **2014**, *21*, 35–48. [CrossRef]
41. Li, J.; Zhao, Y.; Han, L.; Zhang, G.; Liu, R. Moisture variation inferred from a nebkha profile correlates with vegetation changes in the southwestern Mu Us Desert of China over one century. *Sci. Total Environ.* **2017**, *598*, 797–804. [CrossRef] [PubMed]
42. Qu, S.; Wang, L.; Lin, A.; Zhu, H.; Yuan, M. What drives the vegetation restoration in Yangtze River basin, China: Climate change or anthropogenic factors? *Ecol. Indic.* **2018**, *90*, 438–450. [CrossRef]
43. Liu, Y.; Liu, H.; Chen, Y.; Gang, C.; Shen, Y. Quantifying the contributions of climate change and human activities to vegetation dynamic in China based on multiple indices. *Sci. Total Environ.* **2022**, *838*, 156553. [CrossRef]
44. Lin, M.; Hou, L.; Qi, Z.; Wan, L. Impacts of climate change and human activities on vegetation NDVI in China's Mu Us Sandy Land during 2000–2019. *Ecol. Indic.* **2022**, *142*, 109164. [CrossRef]
45. Xu, J.; Xiao, F.; Liao, W.; Wang, G.; Zhou, Y. Spatio-temporal Changes of vegetation and its geomorphic differentiation in the middle reaches of the Hanjiang River based on modis ndvi data. *Resour. Environ. Yangtze Basin* **2017**, *26*, 1895–1901. [CrossRef]
46. Du, J.; Fu, Q.; Fang, S.; Wu, J.; He, P.; Quan, Z. Effects of rapid urbanization on vegetation cover in the metropolises of China over the last four decades. *Ecol. Indic.* **2019**, *107*, 105458. [CrossRef]
47. Hu, Y.; Yu, X.; Liao, W.; Liu, X. Spatio-Temporal Patterns of Water Yield and Its Influencing Factors in the Han River Basin. *Resour. Environ. Yangtze Basin* **2022**, *31*, 73–82.
48. Zhang, Z.; Liang, S.; Xiong, Y. Vegetation Dynamics and Their Response to Climate Changes and Human Activities: A Case Study in the Hanjiang River Basin, China. *Forests* **2023**, *14*, 509. [CrossRef]
49. Yang, S.; Liu, J.; Wang, C.; Zhang, T.; Dong, X.; Liu, Y. Vegetation dynamics influenced by climate change and human activities in the Hanjiang River Basin, central China. *Ecol. Indic.* **2022**, *145*, 109586. [CrossRef]
50. Li, X.; Ren, Z.; Zhang, C. The correlation analysis and space-time changes of NDVI and hydro-thermal index in Hanjiang basin. *Geogr. Res.* **2013**, *32*, 1623–1633. [CrossRef]
51. Liu, H.; Zheng, L.; Yin, S. Multi-perspective analysis of vegetation cover changes and driving factors of long time series based on climate and terrain data in Hanjiang River Basin, China. *Arab. J. Geosci.* **2018**, *11*, 509. [CrossRef]
52. Hu, Y.; Huang, J.; Du, Y.; Yu, X.; Wang, C. Spatio-Temporal Trends of Vegetation Coverage and Their Causes in the Danjiangkou Reservoir Region During 2000 to 2015. *Resour. Environ. Yangtze Basin* **2018**, *27*, 862–872. [CrossRef]
53. Zhang, S.; Ban, X.; Huang, Q.; Liu, D. Analysis of hydrological regime changes in the midstream Han River using range of variability approach. *J. Hydroelectr. Eng.* **2016**, *35*, 34–43. [CrossRef]
54. *GB/T37526—2019*; Assessment Method for Solar Energy Resource. China Meteorological Administration: Beijing, China, 2019.
55. Zhou, C.; Chen, W.; Qian, J.; LI, B.; Zhang, B. Research on the Classification System of Digital Land Geomorphology of 1:1000000 in China. *J. Geo-Inf. Sci.* **2009**, *11*, 707–724. [CrossRef]
56. Cheng, W.; Zhou, C.; Li, B.; Shen, Y.; Zhang, B. Structure and contents of layered classification system of digital geomorphology for China. *J. Geogr. Sci.* **2011**, *21*, 771–790. [CrossRef]
57. Yue, S.; Pilon, P.; Cavadias, G. Power of the Mann–Kendall and Spearman's rho tests for detecting monotonic trends in hydrological series. *J. Hydrol.* **2002**, *259*, 254–271. [CrossRef]
58. Sen, P.K. Estimates of the Regression Coefficient Based on Kendall's Tau. *J. Am. Stat. Assoc.* **1968**, *63*, 1379–1389. [CrossRef]
59. Kendall, M.; Gibbons, J. Rank Correlation Method. *Biometrika* **1957**, *44*, 298. [CrossRef]
60. Mann, H.B. Nonparametric Tests Against Trend. *Econometrica* **1945**, *13*, 245–259. [CrossRef]
61. Hurst, H. Long Term Storage Capacity of Reservoirs. *Trans. ASCE* **1951**, *116*, 776–808. [CrossRef]
62. Wang, X.; Wang, C.; Niu, Z. Application of R/S Method in Analyzing NDVI Time Series. *Geogr. Geo-Inf. Sci.* **2005**, 20–24. [CrossRef]
63. Chu, H.; Venevsky, S.; Wu, C.; Wang, M. NDVI-based vegetation dynamics and its response to climate changes at Amur-Heilongjiang River Basin from 1982 to 2015. *Sci. Total Environ.* **2019**, *650*, 2051–2062. [CrossRef] [PubMed]
64. Yang, S.; Song, S.; Li, F.; Yu, M.; Yu, G.; Zhang, Q.; Cui, H.; Wang, R.; Wu, Y. Vegetation coverage changes driven by a combination of climate change and human activities in Ethiopia, 2003–2018. *Ecol. Inform.* **2022**, *71*, 101776. [CrossRef]
65. Zhang, M.; Wang, J.; Li, S. Tempo-spatial changes and main anthropogenic influence factors of vegetation fractional coverage in a large-scale opencast coal mine area from 1992 to 2015. *J. Clean. Prod.* **2019**, *232*, 940–952. [CrossRef]

66. Wessels, K.J.; van den Bergh, F.; Scholes, R.J. Limits to detectability of land degradation by trend analysis of vegetation index data. *J. Am. Stat. Assoc.* **2012**, *125*, 10–22. [CrossRef]
67. Luo, L.; Ma, W.; Zhuang, Y.; Zhang, Y.; Yi, S.; Xu, J.; Long, Y.; Ma, D.; Zhang, Z. The impacts of climate change and human activities on alpine vegetation and permafrost in the Qinghai-Tibet Engineering Corridor. *Ecol. Indic.* **2018**, *93*, 24–35. [CrossRef]
68. Jin, K.; Jin, Y.; Wang, F.; Wang, S. Impacts of anthropogenic activities on vegetation cover changes in the Circum-Bohai-Sea region, China. *Geocarto Int.* **2022**, *37*, 9339–9354. [CrossRef]
69. Jin, K.; Wang, F.; Han, J.; Shi, S.; Ding, W. Contribution of climatic change and human activities to vegetation NDVI change over China during 1982–2015. *Acta Geogr. Sin.* **2020**, *75*, 961–974. [CrossRef]
70. Wen, Z.; Wu, S.; Chen, J.; Lü, M. NDVI indicated long-term interannual changes in vegetation activities and their responses to climatic and anthropogenic factors in the Three Gorges Reservoir Region, China. *Sci. Total Environ.* **2017**, *574*, 947–959. [CrossRef]
71. Li, S.; Zhang, Y.; Wang, C.; Wang, T.; Yan, J. Coupling effects of climate change and ecological restoration on vegetation dynamics in the Qinling-Huaihe region. *Prog. Geogr.* **2021**, *40*, 1026–1036. [CrossRef]
72. Zhang, L.; Ding, M.; Zhang, H.-m.; Wen, C. Spatiotemporal Variation of the Vegetation Coverage in Yangtze River Basin during 1982–2015. *J. Nat. Resour.* **2018**, *33*, 2084–2097. [CrossRef]
73. Qu, S.; Wang, L.; Lin, A.; Yu, D.; Yuan, M.; Li, C.a. Distinguishing the impacts of climate change and anthropogenic factors on vegetation dynamics in the Yangtze River Basin, China. *Ecol. Indic.* **2020**, *108*, 105724. [CrossRef]
74. Chen, S.; Zhang, Y.; Wu, Q.; Liu, S.; Song, C.; Xiao, J.; Band, L.E.; Vose, J.M. Vegetation structural change and CO2 fertilization more than offset gross primary production decline caused by reduced solar radiation in China. *Agric. For. Meteorol.* **2021**, *296*, 108207. [CrossRef]
75. Wang, Y.; Dai, E. Spatial-temporal changes in ecosystem services and the trade-off relationship in mountain regions: A case study of Hengduan Mountain region in Southwest China. *J. Clean. Prod.* **2020**, *264*, 121573. [CrossRef]
76. Huo, H.; Sun, C. Spatiotemporal variation and influencing factors of vegetation dynamics based on Geodetector: A case study of the northwestern Yunnan Plateau, China. *Ecol. Indic.* **2021**, *130*, 108005. [CrossRef]
77. Keenan, T.F.; Riley, W.J. Greening of the land surface in the world's cold regions consistent with recent warming. *Nat. Clim. Chang.* **2018**, *8*, 825–828. [CrossRef]
78. Tao, J.; Zhang, Y.; Dong, J.; Fu, Y.; Zhu, J.; Zhang, G.; Jiang, Y.; Tian, L.; Zhang, X.; Zhang, T.; et al. Elevation-dependent relationships between climate change and grassland vegetation variation across the Qinghai-Xizang Plateau. *Int. J. Climatol.* **2015**, *35*, 1638–1647. [CrossRef]
79. Xu, X.; Cheng, Y.; Jiang, H.; Li, X.; Liu, Y. Research progress of the effects of wind speed change on grassland ecosystem. *Acta Ecol. Sin.* **2017**, *37*, 4289–4298. [CrossRef]
80. Qi, X.; Jia, J.; Liu, H.; Lin, Z. Relative importance of climate change and human activities for vegetation changes on China's silk road economic belt over multiple timescales. *Catena* **2019**, *180*, 224–237. [CrossRef]
81. Zhang, M.; Chen, F.; Guo, H.; Yi, L.; Zeng, J.; Li, B. Glacial Lake Area Changes in High Mountain Asia during 1990–2020 Using Satellite Remote Sensing. *Research* **2022**, *2022*, 9821275. [CrossRef]
82. Jia, H.; Chen, F.; Pan, D.; Du, E.; Wang, L.; Wang, N.; Yang, A. Flood risk management in the Yangtze River basin—Comparison of 1998 and 2020 events. *Int. J. Disaster Risk Reduct.* **2022**, *68*, 102724. [CrossRef]
83. Yu, B.; Yang, A.; Chen, F.; Wang, N.; Wang, L. SNNFD, spiking neural segmentation network in frequency domain using high spatial resolution images for building extraction. *Int. J. Appl. Earth Obs. Geoinf.* **2022**, *112*, 102930. [CrossRef]
84. Yu, B.; Chen, F.; Ye, C.; Li, Z.; Dong, Y.; Wang, N.; Wang, L. Temporal expansion of the nighttime light images of SDGSAT-1 satellite in illuminating ground object extraction by joint observation of NPP-VIIRS and sentinel-2A images. *Remote Sens. Environ.* **2023**, *295*, 113691. [CrossRef]
85. Yu, B.; Xu, C.; Chen, F.; Wang, N.; Wang, L. HADeenNet: A hierarchical-attention multi-scale deconvolution network for landslide detection. *Int. J. Appl. Earth Obs. Geoinf.* **2022**, *111*, 102853. [CrossRef]
86. Yu, B.; Chen, F.; Wang, N.; Wang, L.; Guo, H. Assessing changes in nighttime lighting in the aftermath of the Turkey-Syria earthquake using SDGSAT-1 satellite data. *Innovation* **2023**, *4*, 100419. [CrossRef]
87. Jia, H.; Chen, F.; Zhang, C.; Dong, J.; Du, E.; Wang, L. High emissions could increase the future risk of maize drought in China by 60–70%. *Sci. Total Environ.* **2022**, *852*, 158474. [CrossRef]